

University of Windsor

Scholarship at UWindor

Electronic Theses and Dissertations

Theses, Dissertations, and Major Papers

1-10-2024

Boat Wake Attenuation through Artificial Vegetation - A Case Study from Peche Island

Jamie Kathryn Lilly
University of Windsor

Follow this and additional works at: <https://scholar.uwindsor.ca/etd>



Part of the [Environmental Sciences Commons](#)

Recommended Citation

Lilly, Jamie Kathryn, "Boat Wake Attenuation through Artificial Vegetation - A Case Study from Peche Island" (2024). *Electronic Theses and Dissertations*. 9151.

<https://scholar.uwindsor.ca/etd/9151>

This online database contains the full-text of PhD dissertations and Masters' theses of University of Windsor students from 1954 forward. These documents are made available for personal study and research purposes only, in accordance with the Canadian Copyright Act and the Creative Commons license—CC BY-NC-ND (Attribution, Non-Commercial, No Derivative Works). Under this license, works must always be attributed to the copyright holder (original author), cannot be used for any commercial purposes, and may not be altered. Any other use would require the permission of the copyright holder. Students may inquire about withdrawing their dissertation and/or thesis from this database. For additional inquiries, please contact the repository administrator via email (scholarship@uwindsor.ca) or by telephone at 519-253-3000ext. 3208.

Boat Wake Attenuation through Artificial Vegetation – A Case Study from Peche Island

By

Jamie K Lilly

A Thesis

Submitted to the Faculty of Graduate Studies

through the School of the Environment

in Partial Fulfillment of the Requirements for

the Degree of Master of Science

at the University of Windsor

Windsor, Ontario, Canada

© 2023, Jamie Lilly

**Boat Wake Attenuation through Artificial Vegetation –
A Case Study from Peche Island**

by

Jamie Lilly

APPROVED BY:

T. Bolisetti

Civil and Environmental Engineering

A. Fisk

School of the Environment

C. Houser, Advisor

School of the Environment

November 13th, 2023

Declaration of Originality

I hereby certify that I am the sole author of this thesis and that no part of this thesis has been published or submitted for publication.

I certify that, to the best of my knowledge, my thesis does not infringe upon anyone's copyright nor violate any proprietary rights and that any ideas, techniques, quotations, or any other material from the work of other people included in my thesis, published or otherwise, are fully acknowledged in accordance with the standard referencing practices. Furthermore, to the extent that I have included copyrighted material that surpasses the bounds of fair dealing within the meaning of the Canada Copyright Act, I certify that I have obtained a written permission from the copyright owner(s) to include such material(s) in my thesis and have included copies of such copyright clearances to my appendix.

I declare that this is a true copy of my thesis, including any final revisions, as approved by my thesis committee and the Graduate Studies office, and that this thesis has not been submitted for a higher degree to any other University or Institution.

Abstract

The use of nature-based solutions and engineering ideas has sparked interest in the value of vegetated shorelines for protecting against erosion. However, there is a lack of field data, and more research is needed to understand how effective vegetation is in reducing the impact of wind waves and boat wakes. The difference in period between wind waves and boat wakes suggests that they may be attenuated differently, requiring further study to determine the optimal management design. The purpose of this study is to quantify the ability of artificial vegetation to attenuate boat wakes and calculate the drag coefficient for model vegetation. The field study was completed on Peche Island in the Detroit River that is estimated to have decreased in area due to the passage of cargo and recreational vessels capable of generating large wakes. Pressure transducers were constructed to track the amount of wave decay occurring between vegetated and non – vegetated transects from boat wakes occurring at the shoreline, these values were calculated for drag coefficients and plotted alongside previous study results. Results suggest that the artificial vegetation was capable of attenuating wakes, but only after the cross-shore variation in wave height was deshoaled to account for the increase in wave height. Using the deshoaled wave heights, the calculated drag coefficient is greater than all previous studied vegetation and did not exhibit the decay observed in other studies of both artificial and natural vegetation. It is believed that the limited variation in drag and a lack of energy decay is due to the vegetation remaining equally rigid over the wake train and not swaying independently in response to the individual waves. In this respect, the artificial vegetation is an effective attenuator of wakes and a total of 3 stalks per m^2 would be required to provide sufficient attenuation. If installed along the length of Peche Island (1.124km) it is estimated that ~33,720 stems would be required at a cost of ~\$505,800 not including the cost of installation and annual maintenance.

Acknowledgements

I would like to express my appreciation to Dr. Chris Houser and Dr. Alex Smith for guiding me throughout the completion of this project. I am also grateful to the Windsor Coastal Group for their advice and support throughout the data collection and writing process. I want to especially thank Ben Chittle for his time, effort and unwavering positive attitude while constructing the pressure transducers; a process that was made more complicated due to Covid – 19 restrictions. Thank you to my previous Professors who taught me to love and seek challenges in my life. Thank you to the staff at RAEON (Todd Ledley, Aaron Fisk) for their generous offer of not only equipment but their time. My deepest appreciation goes to my boyfriend and friends, who helped to keep me focused and dedicated through this journey.

Table of Contents

Declaration of Originality	iii
Abstract	iv
Acknowledgements	v
1. Introduction	1
2. Background and Literature Review	5
2.1 Wake Characteristics	5
2.2 Wave Attenuation by Vegetation.....	11
2.3 Drag Coefficient.....	16
3. Purpose and Objectives	20
4. Study Site	21
5. Methodology	26
5.1 Pressure Transducers.....	27
5.2 Sensor Deployment.....	31
5.3 Artificial Vegetation Deployment.....	31
5.3.1 Day Four Data.....	32
5.4 Vessel Monitoring.....	33
5.5 Data Analysis.....	34
5.6 Drag Coefficients.....	37
5.7 Wind- Wave Energy.....	39
6. Results	39
6.1 Wake Heights.....	43
6.2 Wave Shoaling.....	45

6.3 Decay Coefficients.....	47
6.4 Drag Coefficients.....	49
6.5 Vegetation Density to Provide Shoreline Protection.....	52
7. Discussion	53
7.1 Index Wave Height and Decay Coefficient.....	54
7.2 Drag Coefficients.....	57
7.3 Artificial Vegetation as an Alternative to Hard Engineering Structures.....	60
8. Conclusions	62
References.....	64
Vita Auctoris	70

1. Introduction

Shoreline erosion is an increasingly significant challenge to coastal managers in Canada, impacting budgetary and development decisions by landowners, municipalities, and regional governments (Ricketts et al. 2007). Erosion and deposition are determined by gradients in sediment transport, which are in turn determined by the available supply of sediment (Gittman et al. 2014), the frequency and magnitude of storm activity (Shepherd et al. 2011), variation in wave direction (NRC, 2007) and the implementation of shoreline protection infrastructure (Douglas and Pickle, 1999). In fetch-limited environments transport gradients and shoreline erosion are typically associated with small, short-period wind-waves, but there is increasing evidence that vessel-generated wakes represent an additional source of wave energy (Bilkovic et al. 2017).

Wakes from both cargo and recreational vessels are capable of resuspending sediment that can also be transported cross-shore and alongshore by wave-generated and/or tidal currents (Bilkovic et al. 2017). Resuspended bed sediments can also increase turbidity and degrade water quality in nutrient-rich environments while limiting the growth of aquatic vegetation such as seagrass that requires high minimum light requirements (e.g., 11-20% of surface light) to thrive (Koch 2002; Koch et al. 2006; Rapaglia et al. 2011). At the shoreline, wakes have also been associated with damage to infrastructure and pose a danger to swimmers (Ricketts et al. 2007), with the potential impact dependent on the size, speed and weight of the vessel, and the distance of the shoreline from the sailing line (Bilkovic et al. 2017).

There has been an increasing focus on ‘nature-based’ solutions that are engineered to mimic or recreate natural processes that support a resilient system. While there is concern that the label ‘nature-based’ solutions co-opt Indigenous knowledge and/or is simply an attempt to green traditional engineering practice (Sedden et al. 2020), it has resulted in greater interest in the use of

both natural and artificial vegetation to attenuate waves. (Ozeren et al., 2014). This movement is an attempt to move away from a reliance on hardened shoreline infrastructure (e.g., rockwalls, groins and jetties) that are incapable of migrating in response to lake or sea level changes. Moreover, Armoured shorelines can contribute to erosion directly adjacent to the structure by limiting the availability of sediment and altering sediment transport gradients (Gittman et al. 2015) which can starve downdrift shorelines of sediment. The emplacement of rockwalls can lead to vertical erosion to compensate for the loss of horizontal (shoreline) erosion, potentially undercutting and collapse of the hardened structure that could require reconstruction and replacement over time. Armoured shorelines also generate reflected wave energy, leading to loss of shallow nearshore habitat through downcutting that in turn could cause the revetment being undermined and failing (NRC, 2007).

In contrast to armoured/hardened structures, vegetated (nature-based) shorelines can provide humans with many benefits known as ‘ecosystem services’ (Moëller, 2006) and may represent a cost-effective management strategy that can limit erosion, (Yang et al. 2012) provide habitat for a range of flora and fauna (Moëller et al. 2014), reduce storm surge (Curren et al. 2015), and contribute to water filtration (Francalanci et al. 2013). Additionally, natural vegetation can increase shoreline durability through the development of root systems that bind soil, reduce wave energy, stabilize sediments, and enhance soil quality (Augustin et al, 2009). However, the most important role played by vegetation is its ability to attenuate wind waves and currents (Zang et al. 2022) due to friction between the water and plant stems that is described in terms of a Drag Coefficient (C_D). The result is an attenuation of the wave height as it approaches the shoreline that can be described in terms of a decay coefficient (Bradley & Houser, 2009). Sufficiently dense vegetation can also disrupt the formation and propagation of wind waves by acting as a barrier

which may cause the waves to break earlier and with less energy than in open water. (Curren et al. 2015). In environments where vegetation is not well established or there are limitations to natural growth and extension (e.g., substrate, disturbance, depth), artificial vegetation may provide similar benefits without the need for shoreline hardening.

While there have been numerous studies to quantify the attenuation of wind-generated waves (Passaro et al. 2021), there is a lack of data on how effectively vegetation attenuates vessel-generated waves. Given that wave attenuation depends on depth, wave period and the flexibility of the vegetation, a boat wake with variable (decreasing) frequencies may not be attenuated the same as quasi-steady wind-generated waves. In response to wind-waves, the vegetation sways at a nearly constant phase to the orbital velocities of the wave, with the longest superimposed wave controlling the movement of the stem (Bradley and Houser, 2009). However, boat wakes are characterized by waves of decreasing period, such that the movement of the stem in response to the first wave may influence the movement in response to the next wave. Based on both field and laboratory results (Bradley and Houser, 2009; Houser et al., 2014), it is reasonable to assume that the C_D of vegetation under wakes will be greater due to the out-of-phase movement of the stem with each successive wave in the wake train.

While there is anecdotal evidence to suggest that boat wakes are attenuated by vegetation from the field (Ismail et al. 2017) and the laboratory (Manis et al. 2015), there have been no studies to quantify the ability of vegetation to attenuate unsteady wave trains (e.g., wakes) and quantify the associated C_D of the vegetation. Such measurements can provide insight for coastal managers to better protect shorelines from erosion using vegetation as a living (nature-based) shoreline, or by identifying wake restrictions to limit shoreline impacts based on the extent, density, and type of vegetation (NRC 2007; Shepard et al. 2011; Gittman et al., 2014;).

The size of the wake that reaches the shoreline is dependent on the distance to the sailing line and the characteristics of the vessel. Specifically, wakes dissipate through dispersion as they move away from the sailing line, meaning that the smaller a wave is at the onset, and the farther from the shoreline is generated, the less wave energy will arrive at the shoreline. Given that the size of the waves in a wake also depend on the size, speed, and weight of the vessel, as well as the way in which the boat is being driven (plowing versus planning), the height and period of a wake at the shoreline can be highly variable. This in turn makes it difficult to determine the relative importance of boat wakes to shoreline change and there is little data regarding shoreline position and the natural rate of shoreline change before the introduction of boat traffic. This means that there is a lack of ‘control’ data to quantify the amount of shoreline change due to boats or to assess their impact on water quality (Galmore 2008). In many jurisdictions around the world, the impact of boat wakes is mitigated through speed limits at a given distance from the shoreline or within narrow waterways (NRC,2007). However, speed limits are largely based on safety and do not consider the potential for wakes based on the way in which the boat is driven (plowing versus planning) or the depth of water. Except for enforced no-wake zones, it is not possible to limit wake heights by limiting boating activity, such that mitigation strategies are required to limit shoreline change in fetch-limited environments (Galmore, 2008).

2. Background and Literature Review

2.1 Wake Characteristics

Wakes are generated by the forward movement of a boat along the water's surface and the displacement of the water surface by the vessel. The forward movement of the vessel creates symmetrical (bow) waves that propagate away from the bow at an oblique angle, while the water displacement creates a stern wave that is sometimes called a transverse wave (Figure 1, Figure 2). The size of the bow wave depends on the amount of water pushed forward by the vessel, which in turn depends on the speed of the vessel and how it is driven (plowing versus planning, (Figure 3), with the largest waves generated by wake boats that are designed to plow at high speeds. The size of the stern wave depends on the weight of the vessel, which determines how much water is displaced and needed to be restored after the vessel has passed. Bow waves interact with stern waves at a point known as the cusp, where maximum wave height is achieved. Any waves that fall between the cusp points are smaller than the maximum wave height, resulting in a complex series of high frequency waves referred to as a wave train.

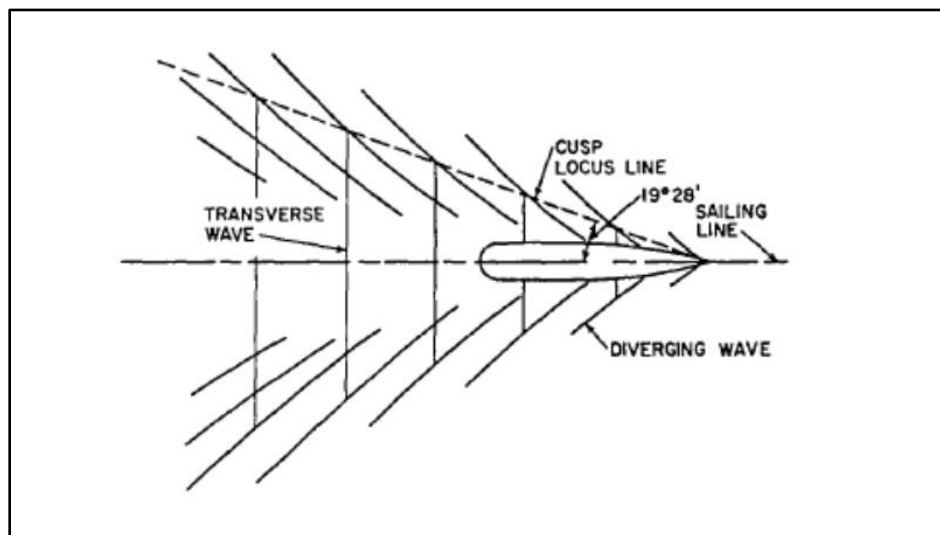


Figure 1: Propagation of vessel generated waves in deep water. Modified from "Review of boat wake wave impacts on shoreline erosion and potential solutions for the Chesapeake Bay" by Bilkovic et al. 2017.



Figure 2: Photo of a vessel in forward motion creating symmetrical bow waves that interact with stern waves at the cusp line as they move away from the vessel. Photo courtesy of C. Houser

As noted, the size of the bow and stern wakes depends on the speed and length of the vessel, which is described through the Froude (Fr) number (Hager and Orgaz, 2016). The Fr is a dimensionless parameter to describe the ratio of the inertial forces (velocity) to gravitational (or restoring) forces in a fluid. Boat wakes are described through both the length-based Fr (Fr_L) and the depth-based Fr (Fr_d), which describe the interaction of the bow and stern wakes, and the size of the bow wake respectively. The Fr_L is calculated as

$$(Fr_L) = \frac{(V)}{\sqrt{g * L}} \quad (1)$$

Where V is the velocity of the boat relative to the water, g is the acceleration due to gravity and L is a characteristic length, often the length of the boat. (Hager and Orgaz, 2016).

At $Fr_L=0.5$, the 7 interaction of the bow and stern wakes (at the cusp) construct to create the largest maximum wave for a given vessel, while $Fr_L<0.5$ and $Fr_L>0.5$ results in limit interaction and smaller waves. The Fr_d is calculated as:

$$Fr_d = \frac{(V)}{\sqrt{g * h}} \quad (2)$$

where h is the depth of the water and $\sqrt{g * h}$ is the speed of a wave in shallow water. When $Fr_d = 1$, the speed of the vessel is equal to the speed of the bow wave, leading to the continuous addition of energy to the developing wave. When $Fr_d < 1$, the vessel pushes through the bow wake before it is fully developed.

The displacement and resulting wake size also depend on the shape of the hull (e.g., planing hull) (Figure 3) and the way the vessel is driven (Baldwin,2008). Planing hulls, common on recreational vessels, create the smallest waves that increase with increasing vessel speed when operating in displacement mode (flat on water and slow). As the vessel speed increases, the bow lifts out of the water and the boat begins to plow through the water, leading to increasingly large bow wakes. A further increase in speed pushes the vessel into planing mode as the bow returns flat to the water surface leading to a reduction in wake height from the maximum under plowing (Bilkovic et.al, 2017). Displacement hulls, common on sailboats, trawlers, and cargo ships are designed to ride in the water, pushing the bow wake to the side as the vessel moves forward. In general, planing hulls generate larger bow waves and smaller stern waves as compared to displacement hulls (Figure 3).

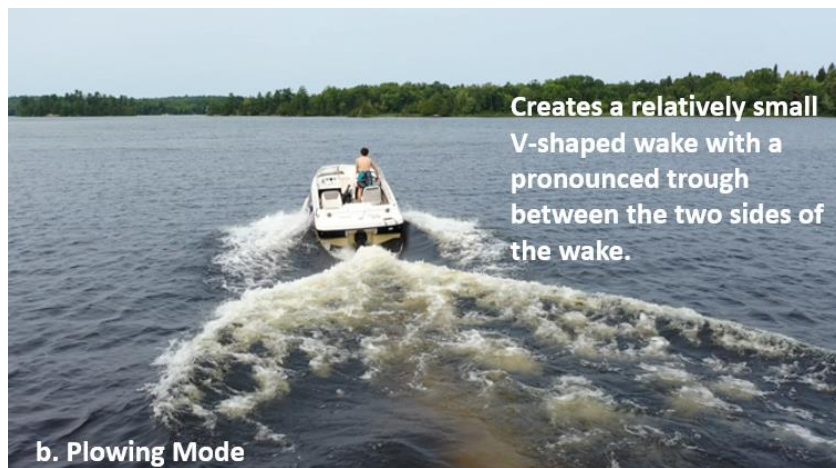


Figure 3: Vessel mode of operations and their respective wake characteristics: a. Displacement mode b. Plowing mode c. Planing mode. Photo courtesy of C. Houser

In addition to the wakes generated at the bow and stern, the acceleration of flow beneath the vessel causes a drawdown of the water surface around the boat. The larger and heavier the vessel (e.g., cargo vessel), the greater the drawdown as the vessel passes. Behind the vessel, a transverse stern wave travelling in the same direction as the vessel raises water levels to compensate for the drawdown- this raise in water level can inundate adjacent shorelines (Houser, 2010). The amount of drawdown depends on the ratio of the ship cross-sectional area to the cross-sectional area of the channel, and when this blockage ratio increases, vessels can generate larger drawdown and return current velocities that can erode the shoreline (MacDonald, 2003; Houser et al. 2010). The remainder of this thesis will focus on the shorter-period bow and stern waves, and not the long-period drawdown wave that is not attenuated at the shoreline and is more akin to an infragravity waves.

In addition to the vessel design, speed and displacement, the height and period of a wake at the shoreline is dependent on the navigation channel characteristics including shape, width, and tidal regime (Galmore, 2008). For instance, wider channels allow waves to spread out more, resulting in a decrease in wave height and longer wave periods. Narrower channels can lead to higher wave heights and shorter wave periods as the waves are compressed within the restricted space (Galmore, 2008). In shallower channels, waves may interact with the channel bottom, causing wave energy to be transformed into turbulent motion or breaking waves, which can decrease wave height and increase wave period. Deeper channels generally allow waves to propagate with less interaction with the channel bed, potentially resulting in higher wave heights and longer periods (Galmore, 2008). Ultimately, the overall impact to the shoreline is dependent on the number of vessels that pass the nearshore (Ahmed et al. 2011). The cumulative effect of

numerous boat wakes over time can contribute to the overall wave energy budget in the nearshore region, this is particularly true in areas with high boat traffic or confined water bodies (Ahmad et al. 2011).

As a wake moves away from the sailing line, the longer period waves travel faster than the smaller period waves through a process called dispersion leading to a decrease in wake height as the waves separate. As a result, a wake approaching the shoreline starts with lower frequency (longer period) waves followed by increasingly short period waves. (Figure 4). The decay in wave height away from the sailing line can also occur through dispersion frictional losses due to viscosity and interaction with the bottom in shallow environments. The combination of dispersion and frictional losses leads to an exponential decay in wave height 10 away from the sailing line, such that the size of the wake waves that reaches the shoreline will depend on its distance to the sailing line, along with the specific size of the vessel and speed of travel. (Soomere, 2007; Houser, 2010; Bilkovic et.al,2017)

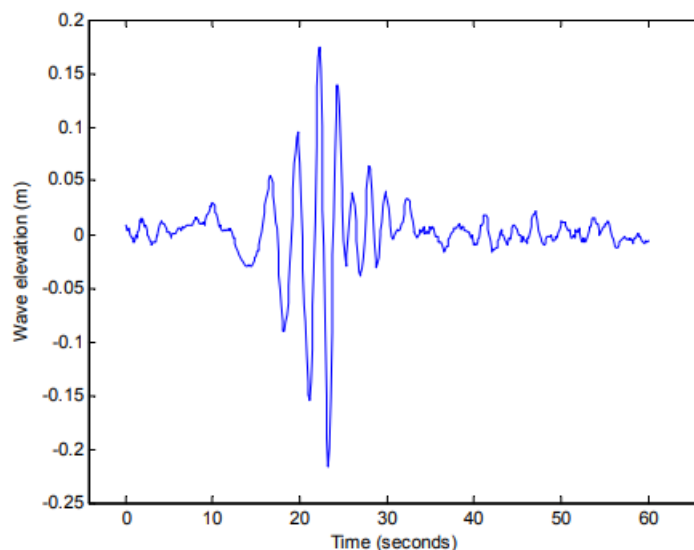


Figure 4: Measured wave profile showing the initial small height and long period of the boat wake, followed by waves of large height and moderate period (From Newman, 1977).

As waves enter depths of less than $\frac{1}{2}$ their wavelength (i.e., the distance between crests), they begin to shoal as the lowermost orbits extend to and interact with the bottom. During shoaling, wave heights increase through the conservation of energy as the wave speed and wavelength decrease. Due to shoaling, the wave height at some point in the nearshore (H_n) can be expressed as:

$$H_n = K_s H_o \quad (3)$$

where H_o is the offshore wave height and K_s is the shoaling coefficient that depends on the wave period and water depth. Combined with frictional losses due to the presence of vegetation (Section 6.2), the H_n can be expressed as:

$$H_n = K_s K_f H_o \quad (4)$$

where K_f is the frictional coefficient that depends on the characteristics of the vegetation including width, flexibility, and height. When K_s is greater than K_f , the wave will grow despite the presence of vegetation up to the point at which the wave height is ~80% of the depth and the wave breaks. Consequently, wakes approaching the shoreline will increase in size up to the breakpoint in shallow water before decreasing in height due to breaking (Parnell & McDonald, 2007; Bilkovic et al., 2017). As most boat wakes have a period (and wavelength) longer than locally generated wind waves, wakes tend to break at or very close to the shoreline in dissipative (flat) nearshore environments or simply surge where the beach is relatively steep (i.e., reflective).

2.2 Wave Attenuation by Vegetation:

Numerous studies have examined the attenuation of wave energy with emergent vegetation (Knutson et al. 1982; Cooper, 2005; Löfstedt and Larson, 2010) submerged vegetation like seagrass and kelp (Bradley & Houser, 2008) (Mork, 1996) and artificial vegetation in the

laboratory (Lima et al. 2006; Augustin et al. 2009, Regardless of vegetation type, the resulting wave height decay through vegetation is described as an exponential function:

$$\frac{H_2}{H_1} = e^{-k\Delta x} \quad (5)$$

where H_1 and H_2 are wave heights at shore-normal positions separated by Δx and the exponent k_i is the decay coefficient. Depending on the characteristics of the vegetation, the decay coefficient can vary from 0.01 (Moller et al, 1999) to 0.05 (Kobayashi et al. 1993) and reach as high as 0.10 (Mendez et al.1999). Studies show that emergent salt marsh vegetation can decrease wave energy up to 3.1% per meter over 30 meters (Knuston et al. 1982). While in in emergent reeds (*Phragmites australis*) an average decrease in wave height of 4-5% per has been observed (Lövstedt and Larson, 2010). Cooper (2005) found that wave attenuation over salt marshes with emergent conditions was at least two times greater than over mudflats, with the highest wave reduction at 0.30% per m (Cooper, 2005). Within submerged vegetation studies, kelp beds show a reduction in wave height by 60% over 258 meters (Mork, 1996) and submerged seagrasses showed a 0.77% decrease in wave height per meter over 39 meters (Bradley & Houser 2008). Vegetation-wave interactions have also been studied under controlled conditions in laboratory flume studies. Lima et al. (2006) tested the effects of nylon rope and reported attenuation values of 5% per m for 600 stems/m² (Lima et al. 2006); while Augustin et al. (2009) used cylindrical wooden dowels and observed 50-200% greater wave attenuation per wavelength over emergent than near emergent vegetation.

Table 1: Field and laboratory studies of wave attenuation over vegetation and their average wave reductions.

Reference	Transect Length (m)	Vegetation Type	Average Wave Reduction (% m)
Lövstedt and Larson, 2010	Over first 5-14 m of vegetation	Semi-Emergent Seagrass	4.0-5.0
Cooper, 2005	300	Semi-Emergent Seagrass	0.30
Knutson et al. 1982	30	Emergent	3.1
Bradley & Houser, 2008	39	Submerged Seagrass	0.77
Mork, 1996	258	Submerged Kelp	60
Augustin et al. 2009	30.5m wave tank	Artificial- Emergent	50-200 (per wavelength)
Lima et al. 2006	43m wave tank	Artificial- Submerged	0.83-1.67

The differing results between these studies reflects how attenuation is influenced by the height/length of the vegetation, density of the plant field, stem rigidity, flexibility, hydrodynamic controls of the waves on the individual stalks of vegetation, as well as the size and density of the marsh (Bradley & Houser, 2009). The drag (resistance) that occurs over vegetation in water is primarily a result of the interaction between the flowing water and the physical structure of the vegetation and is largely responsible for its attenuation capability (Augustin et al, 2009).

Vegetation in water, such as submerged plants, aquatic grasses, and emergent reeds, has physical structures that extend above and below the water's surface. These structures create obstacles that the water has to flow around, leading to a change in the flow pattern (Anderson and Smith, 2014). As water flows towards the vegetation, it encounters the vegetation's stems, leaves and other parts. These parts can cause the flow to separate, leading to eddies and vortices forming downstream. This separation of flow creates areas of lower pressure behind the vegetation, contributing to drag. Maximum drag and attenuation are realized when (emergent) vegetation extends to and above the water surface (Augustin et al. 2009), with decreasing drag and attenuation

for submerged vegetation such as seagrass (Bradley & Houser, 2008). Submerged parts of the vegetation can create additional resistance, contributing to attenuation, and the arrangement (or density) of vegetation can cause interference and increased drag in the flow patterns of water as it moves through the vegetation (Nepf & Ghisalberti, 2008).

In a study involving *Zostera noltii* (known by the common name of dwarf eelgrass) Paul & Amos (2010) show that a minimum stem density was required before attenuation could occur, and that the existence of such a threshold suggests a nonlinear relationship between the two parameters. Moreover, this density threshold varied with hydrodynamics in that higher wave periods resulted in lower shoot density requirements for attenuation. For example, *Zostera noltii*, is a small seagrass with ribbon shaped leaves measuring 0.5-1.5 mm wide and 6-22 cm long, and the fact that a dependence on plant characteristics as well as hydrodynamics can be observed in such a small species of seagrass suggests it may occur in larger species as well. (Paul & Amos, 2010). Dense vegetation such as marshes and mangroves tend to be more effective at absorbing and dissipating wave energy compared to sparse or low-lying vegetation; however, aquatic vegetation that grows underwater such as seagrasses, kelp and some algae can significantly reduce wave energy due to the complex flow interactions between water and vegetation (Grizzle et al. 1996).

Hydrodynamic studies with steady unidirectional flows and vegetation suggest that interactions between the cylinders also affect the overall resistance provided by vegetation (Anderson et al. 2011); while variations in the vegetation fields geometry and spatial coverage can also change the attenuation capacity of a vegetation field (Irish et al. 2008). A laboratory study on modeled emergent vegetation by Nepf (1999) found that attenuation decreased as stem density increased because of turbulence-scale wake sheltering. Wake sheltering is caused by an interaction

between upstream and downstream vegetation whereby upstream vegetation stem wakes reduces the attenuation on downstream stems (Nepf 1999).

Emergent and flexible vegetation, like reeds and cattails can bend and sway in response to wave action; the longer stems from emergent vegetation create more overall drag and friction against the movement of water (Dubi and Tørum ,1996). This leads to increased turbulence and mixing of water within the vegetation, which in turn causes wave energy to be dissipated. The stems essentially act as obstacles that break up the coherent wave motion and transform it into turbulent flow patterns (Fonseca and Cahalan,1992). A study by Tschirky et al. (2000) tested emergent wetland plants within a laboratory setting. Results showed that larger water depths resulted in larger wave transmission (i.e., less attenuation) because the waves were influenced less by the flume bottom (friction) and interact with the thinner, more flexible upper portions of the bulrushes (Tschirky et al. 2000).

2.3 Drag Coefficient

The ability of vegetation to attenuate waves can be expressed through the drag coefficient (C_D), which is a fundamental parameter that influences wave attenuation in water bodies with the presence of vegetation. Vegetation with larger C_D result in more effective dissipation of wave energy (Nepf & Ghisalberti, 2008). The C_D imposed by aquatic vegetation can either be described for an entire patch of vegetation (an effective drag) or for the individual stalks. In general, the drag coefficient decreases as a power function with the Reynolds number (Re) which describes the amount of turbulence over an objects surface and is useful for determining the type of flow around vegetation in response to the passive waves. Drag is greatest under laminar flow (low Re) but decreases as the flow separates around the vegetation stem and the skin drag is minimized. The

roughness or texture of the vegetation, as well as the speed and viscosity of the fluid, can all influence the magnitude of skin drag friction. (Houser et al. 2014). The flow of water around a vegetation stalk can induce turbulence from the shear forces and vortices created as water flows past the stalk; and the intensity and characteristics of stem scale turbulence depend on the flow velocity, shape of the stalk and presence of nearby vegetation. In some cases, flow separation can occur when water flows around a vegetation stem and detaches from the surface of the stalk, creating a wake region which reduces overall drag and can lead to increased drag and changes in the pressure distribution around the stalk (Figure 5).

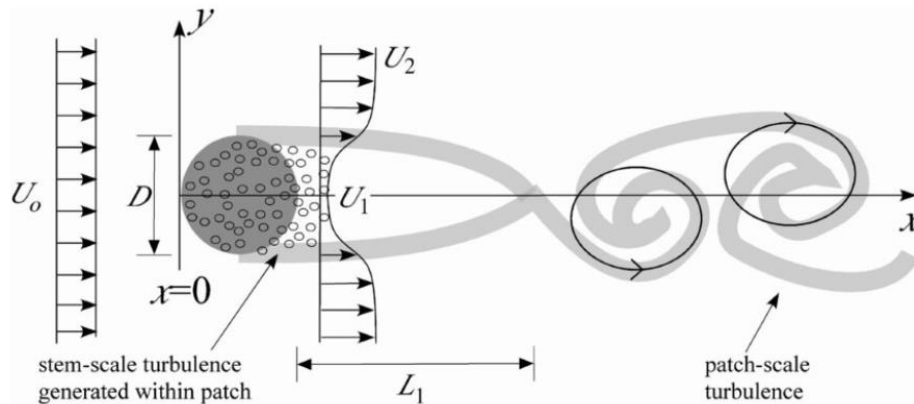


Figure 5: Top view of a circular patch of emergent vegetation with patch diameter D , and upstream, open-channel velocity U_o . (Skin drag). The stem scale turbulence generated within the patch quickly dies out behind the patch. While the flow (form drag) coming through the patch (U_1) blocks interaction between the shear layers at the two edges (Modified from Hydrodynamics of Vegetated Channels (Nepf. 2012)).

Both the drag coefficient and Reynolds number play important roles in understanding wave attenuation and vegetation interaction. The drag coefficient affects how much wave energy is lost when waves encounter vegetation, and the Reynolds number helps predict the type of flow around vegetation and its impact on wave attenuation. (Nepf, 2012). Most studies that have quantified the drag coefficient of vegetation have been carried out in laboratory settings using arrays of rigid or flexible cylinders to represent vegetation (e.g., Augustin et al., 2009, Houser et al. 2014), although there have been some studies conducted with real vegetation in the field

(Bradley & Houser, 2009) and in the flume (Lima et al. 2006). In the study by Augustin et al. (2009), emergent artificial vegetation was tested both for density, drag, turbulence and diffusions

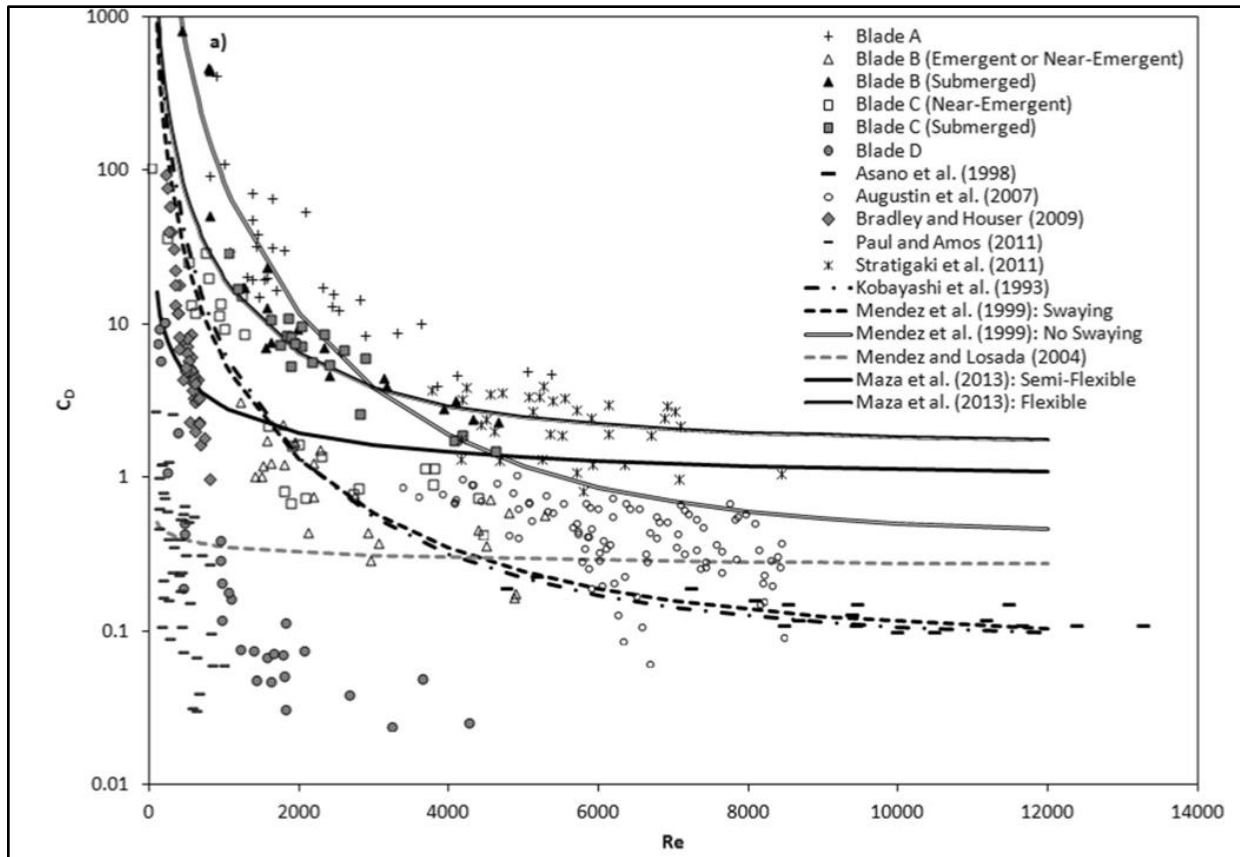


Figure 6: Variations in the drag coefficient among artificial vegetation data and previously published data exhibiting a statistically significant variation with rigidity (From Houser et al. 2014).

and stem height to water ratio. Finding that drag effects were distributed throughout the water column; therefore, wave velocities were impacted along the entire vertical velocity profile. In contrast, submerged conditions resulted in a portion of the water column to be unobstructed by the plant stems, allowing the water to flow freely above the vegetation, resulting in less wave attenuation.

Houser et al. (2014) conducted a study to quantify the influence of blade rigidity and flexibility of the drag imposed by the individual blades of submerged vegetation over a range of wave periods, heights, and water depths. Results indicate that greater flexibility resulted in a

smaller drag coefficient independent of water depth, and the dependency of the drag coefficient on rigidity provides a means to estimate energy dissipation by vegetation of a given blade morphology (Figure 6). Alternatively, the results of Augustin et al. (2009) suggest that the drag would decrease as the depth of the water exceeded the length of the vegetation. Consequently, flexible submergent vegetation provides little to no shoreline protection and ecological stability, except where the vegetation field is extensive and has a relatively large density. This is due to flexible vegetation's capability to 'go with the flow,' resulting in smaller effective blade length and canopy height (Bradley & Houser, 2014). Similarly, Bradley and Houser (2009) found that lower frequency (i.e., longer period) waves could move the entire stem out-of-phase with the shorter frequency waves that only occurred at the top portion of the wave.

The results of past field and laboratory studies have been conducted in single-peaked or quasi-steady wave fields and are not necessarily applicable to unsteady wakes that transition from low frequency (long period) to high frequency (short period) waves such as boat wakes. Based on these previous studies, if the first wave in the wake causes the stalk to sway to an extent allowed by the rigidity of the vegetation, the stalk is bent over further than would be possible with the next wave in the train. This would create a larger 'effective' drag that would be greater than experienced if the waves were all the same period and moved the vegetation the same amount. This effective drag would be greatest for semi-rigid vegetation that can move but does not necessarily 'go with the flow' with every wave (Bradley and Houser, 2014).

3. Purpose and Objectives

This study aims to determine the efficacy of implementing vegetation to attenuate boat wakes within the Detroit River. The objectives of this study were:

- A. Quantify the ratio between vegetation flexibility and wave energy, including attenuation parameters to determine the relative boat wake attenuation between the study arrays and the model control (i.e., with no artificial vegetation present).
- B. Assess calculated drag coefficients against the Reynolds number for artificial stems relative to previously published field and laboratory studies data to determine the optimal density requirements for artificial vegetation and the economic feasibility of this approach as a viable coastal management strategy.
- C. Estimate the minimal artificial vegetation density required to reduce boat wake heights on the Peche Island shoreline and provide an approximate estimation for artificial vegetation implementation to the background wind-wave heights.

4. Study Site

Due to the regular and diverse wake activity and easily accessible shoreline, artificial vegetation was placed along Peche Island in the Detroit River to assess wake attenuation. The area of study is located within the Detroit River which extends 51.5 km from its head at The Windmill Point light, to its mouth at the Detroit River Light in Lake Erie. As water flows out from Lake St. Clair, it is divided by Peche Island; a remanent sedimentary feature in the center of the river. Deep channels on the west side of the island do not naturally allow for the growth of shoreward vegetation fronting the main transportation channel (US Army Corps of Engineers, n.d).

Peche Island covers 32 hectares and is a site of historical importance to Windsor as it was purchased in 1883 as a summer home by the son of Hiram Walker, a multi-generational Windsor family name responsible for the creation of the Hiram Walker and Sons distillery, whose operations are still ongoing today. In 1999 the city of Windsor purchased Peche Island as a municipal park, is accessible by boat and now considered a provincially significant wetland. Between 1931 and 2015, it is estimated that Peche Island has decreased in area by 7 hectares due to the current of the Detroit River, waves from Lake St Clair and a lack of a modern sediment supply (DRCC, 2007). Erosion of the site is episodic and dependent on storm waves and elevated water levels from Lake St Clair (US Army Corps of Engineers, n.d) that also tend to be seasonally greater during the summer season. These storm-scale and seasonal variations in water level and wave activity, are in addition to wakes from cargo and recreational vessels that move through the Lake Erie-Huron corridor. Combined and due to the remnant nature of Peche Island, it is eroding at an increasingly faster rate (DRCC, 2007). Winter lake ice is another potential contributing factor to the erosion of Peche Island, both in its presence and its absence. At the mouth of the Detroit River, near Peche Island, an ice arch from Lake St. Clair develops and attaches itself to either side

of the island. In late winter or early spring, this ice arch retreats into Lake St. Clair, causing large sheets of ice to drift downstream and against the island's shoreline. This shorefast ice and subsequent drift can lead to shoreline erosion along the length of Peche Island (US Army Corps of Engineers, n. d). However, the erosion caused by ice may be less than the erosion resulting from the lack of lake ice with a warming climate and the increase frequency of storm waves capable of developing on Lake St. Clair (Detroit River Shoreline Manual, 2014).

In 2011, a shoreline assessment of Canadian mainland properties within the Detroit River area was conducted to create an inventory and assess shoreline structures and conditions (Detroit River Shoreline Manual, 2014). This study determined that more than 80% of the shoreline length has been developed for urbanization. This has resulted in a large majority of the developed properties requiring artificial hardening. When shorelines are hardened it can result in a direct loss and fragmentation of the natural habitat along the Detroit River shoreline. (Detroit River Shoreline Manual, 2014). The first shoreline protections were constructed along Peche Island in 2022- this was the largest erosion mitigation and fish habitat project on the Canadian side of the Detroit River to date, costing ~ 4.8 million dollars. The project consisted of a shoreline revetment of gabion stone and armour rock on the northeast side of Peche Island, and nine sheltering islands on the north side of Peche Island (Figures 7 &8).

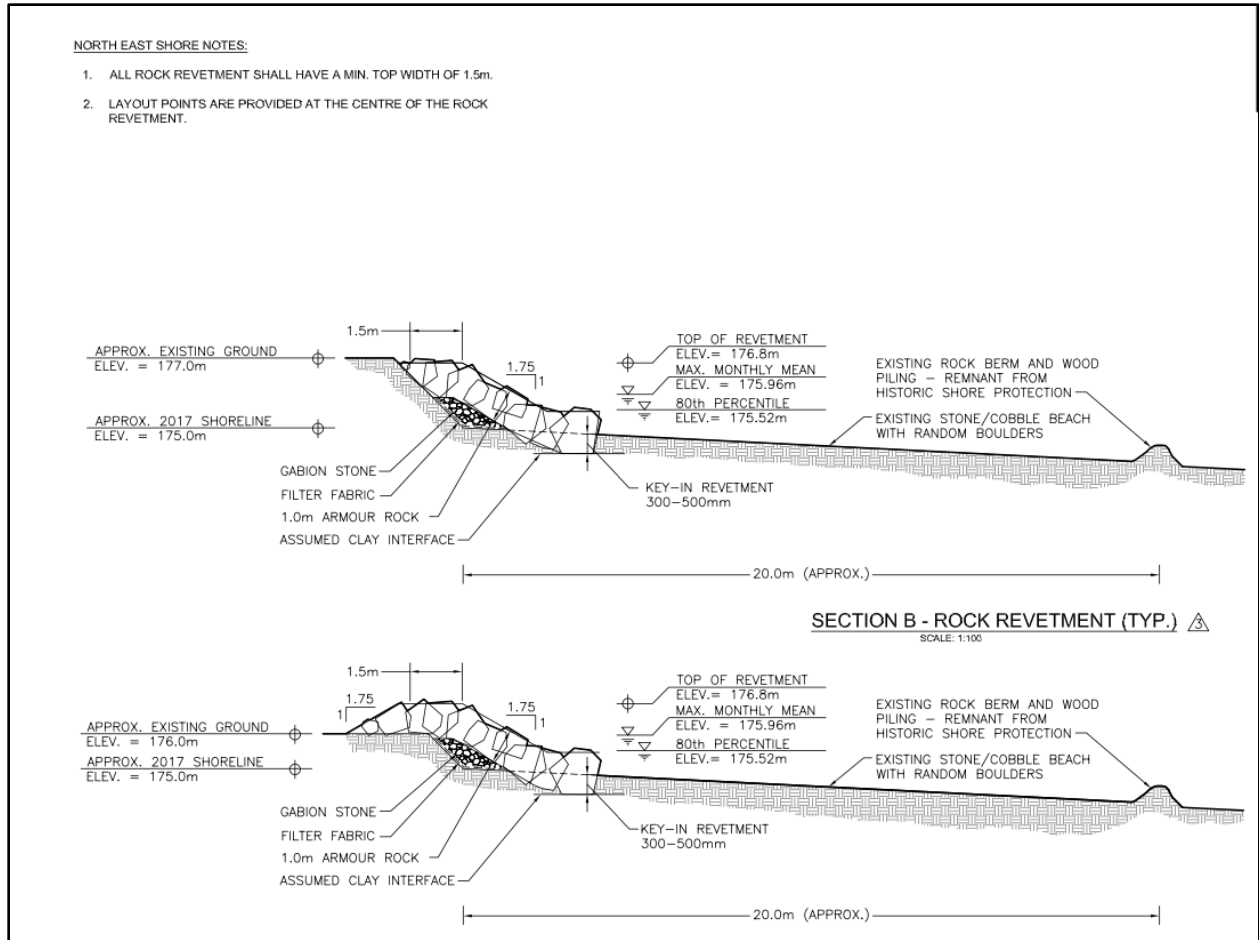


Figure 7: Rock revetment plan and material listing for Peche Island revetment (DRCC Annual report 2021-2022).

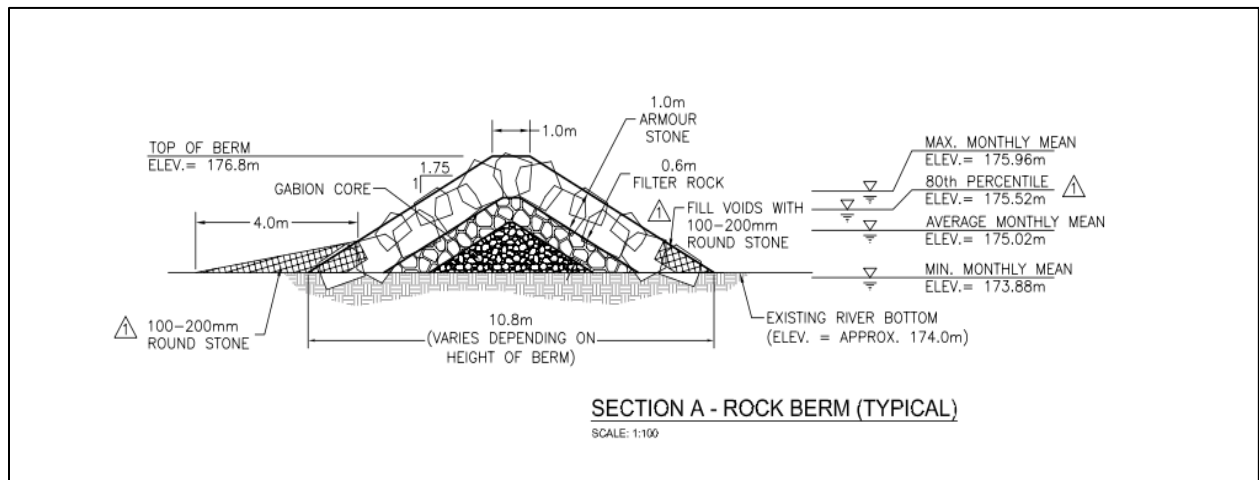


Figure 8: Cross section of proposed berm materials (DRCC Annual Report, 2021-2022).



Figure 9: Engineering plans showing location and spacing of offshore berms (DRCC Annual Report, 2021-2022).

The Detroit River is culturally and ecologically significant, as within the traditional territory of the Three Fires Confederacy of First Nations (Ojibwa, Odawa, and Potawatomi) and was historically used to sustain indigenous peoples (Jacobs & Lytwyn, 2020). More than half of Ontario’s population resides within the shorelines of the Great Lakes and connecting river systems and channels. With the vast economic reliance on shipping through the Detroit River system, considerable strain has been placed on this limited and fragile resource. By implementing offshore islands on the north side of Peche Island for erosion mitigation, calm water embayment is created, that can offer fish refuge and macrophyte habitat to establish (Figure 9).



Figure 10: Aerial imagery of Peche Island, with research location highlighted in red. Google Earth 2023

The sensor and artificial vegetation deployment was located on the section of the shoreline that is southwest of the berms. The specific location (Figure 10) was chosen prior to data collection because it had the largest amount of beach surface area while still facing the international shipping channel. The Peche Island Restoration and Erosion Mitigation project was underway during the time of testing, which limited the amount of shoreline that could be accessed. However, this did not impede data collection or transportation access for the field team.

5. Methodology

Artificial vegetation was installed along 60 meters of the shoreline of Peche Island extending 10 meters out into the channel. Wave energy from wind and boat wakes were measured with pressure transducers that were placed in three transects at 2 meters apart. Transect 1 contained no vegetation and served as a control, while varying vegetation arrays and spacings (Table 3) were placed between sensors on transects 2 and 3. Observable vessel features such as type and speed were recorded in the field along with the time they passed Peche Island and when the wake reached the transects. A mobile application named ‘Marine Traffic’ was then used to cross reference the time of vessel passage with the characteristics of the vessels. Wake information was then extracted from the pressure readings by visual selection and cross referenced with recorded times of vessel passages.

Table 3: Summary of each day's vegetation array and collection times and field conditions.

Date & Collection Time	Spacing (cm)	Configuration	# of Vessels Documented	Wind Speed(km/h) & Direction (10's of degrees).
September 6 th 8:00a.m- 1: 30p.m	80cm from 11:37, then down to 40cm at 12:10.	Linear	75	26.63km/h 12.57°
September 7 th 8:15a.m-12: 45p.m	6 poles at 40 cm apart on 20m transect. 12 poles at 80cm on 45m transect.	Staggered	33	20.05 km/h 17.48°
September 8 th 8:05a.m- 1: 05p.m	6 poles at 40cm apart on 20m transect. 12 poles at 80cm apart on 45m transect.	Staggered	25	21.04 km/h 26.5°
September 9 th 9:00a.m- 11:45p.m	45m transect moved beside 20m transect, 88 poles spaced at 10cm randomly at 45-degree angle.	Randomized	25	15.19 km/h 30.88°

5.1 Pressure Transducers

Commercial instruments that are designed to measure wave forcing can be expensive, especially if the studied area is extensive or deployed in areas where they can be lost. Furthermore, higher access to low-cost sensors allows researchers to perform direct wave climate assessments while increasing the spatial resolution of wave climate data (Temple et al., 2020). These factors led to the decision to build ‘in-house’ pressure sensors by following various publications and altering the electrical and housing components to suit the research requirements. Three different models referred to as MS1, OWHL (also referred to as Boston) and MS2 (which is a combination of MS1 and the OWHL components) were tested and compared. For much of the housing, the guide from Temple et al. (2020), whose approach attempts to seek a balance between accessibility, utility, and practicality was followed.

Materials for housing are readily available at home improvement stores, while being made fully waterproof except for the pressure-sensing element of the sensor. All sensors were constructed from common polyvinyl chloride (PVC) plumbing parts, with a standard 7.62cm diameter pipe separated into 25.4cm lengths. This 25.4cm portion served as the main body, while also housing the sensitive electrical components. A 7.26 cm diameter cap permanently seals one end of the housing pipe while also providing a base for the sensor component. A 3.81cm diameter pipe was cut to 3.175cm length and glued to the center of the cap using PVC cement. This provided some structural protection for the exposed sensor area. A 1.27cm hole is drilled through the cap and into the center of the 3.81cm diameter pipe; allowing for the sensor wires to be fed to the electrical components within the main housing pipe. Using epoxy putty, the wired sensor is set within the smaller pipe on the flat cap; epoxy sealant is then poured evenly over the sensor, sealing the electrical components but leaving the sensor element exposed. A removable 7.62 cm Oatey

Gripper Test Plug provides access to the mechanical components while providing a water-tight seal without cement glue or epoxy. This model by (Temple et al. 2020) was built around Arduino hardware components to control the reading and logging of sensor data through time, namely an Arduino Uno microcontroller.



Figure 11: a. Wired Arduino kit soldered to the exposed sensor board. b: Top of the housing showing the actual sensor set in epoxy. c. Final model used for testing alongside prototypes.

It was discovered that the Arduino kit consumed power at a higher rate than desired, meaning that the battery life would not meet our needs for testing in the field. It was then decided to modify the code associated with this sensor and found that it still was not enough reduction. This led to the decision to move from the Arduino kit to the Arduino chip (ATmega328p), finding that this did reduce power consumption significantly. It was further discovered that the Open Wave Height Logger (OWHL) model by (Theodore et al. 2020) also used the ATmega328p chip. OWHL used a generic microSD card slot and the DS3231S chip for

their clock which helped reduce power consumption. Generic breakout boards were used for the SD slot to modify them to work at 3V instead of 5V, and a generic DS3231 breakout board for the clock which we modified by removing an LED and the circuit to charge the clock battery. Where the OWHL used PCBs (printed circuit boards) to solder electronics onto, the electronics for the MS2 model were hand-soldered onto small breadboards. In terms of programming, all three models sampled at different intervals. MS1 samples continuously as fast as possible, until there was no longer power available. OWHL sampled ~16 times per second. MS2 sampled for 17 minutes and slept (powered down) for 3 minutes, and then repeated. All three models save data into a CSV file with slightly different formatting, the OWHL and MS2 create a new CSV each day at midnight for long- term sampling.

All three models were tested alongside an RBR- TWR2050 sensor, which is commercial grade pressure sensor used to track water parameters such a temperature, depth, salinity, pH and many others within professional and academic settings. The RBR-TWR-2050 is self-contained and compact (265mm length). It operates on two type 123 lithium camera batteries and is equipped with an 8 Mbyte flash memory for data storage. This configuration allows for ample power and storage for deployments of up to two months. The RBR TWR-2050 sampled at 1Hz and sampled continuously alongside the tested sensors. The comparison test was conducted in a 7.31m diameter pool, with an average of 1.67m depth. Wave activity was simulated for thirty minutes, and it was found that the wave frequencies of each model followed the RBR- TW2050 with slight variations in the peak spectra between the models (Figure 12). Significant wave heights were then taken for each sensor for weak wave sets, full depth wave sets, high frequency large wave sets, and high frequency small wave sets (Table 2), which shows that the depth and wave heights are more closely matched by the MS2 then the other models. The RBR-TWR2050 measured a depth of 1.55 meters

within the pool with MS1 at 1.69m, MS2 at 1.61m and OWHL at 1.64m. The RBR-TWR2050 measured a maximum wave height of 0.71, with MS2 containing the closest measurement at 0.75. The smallest wave recorded by the RBR -TWR2050 was 0.44m, however both the MS2 and OWHL measured 0.46mm. The MS2 sensor most closely followed the RBR-TWR2050 significant wave height measurements, and when compared to MS1 the MS2 sensor consumed power at a lesser rate, thus contained longer battery life. While the OWHL sensor housing was more robust and efficient, assembly was difficult, and parts were difficult to obtain due to COVID-19 restrictions. These factors combined led to the decision for choosing the MS2 model for this study.

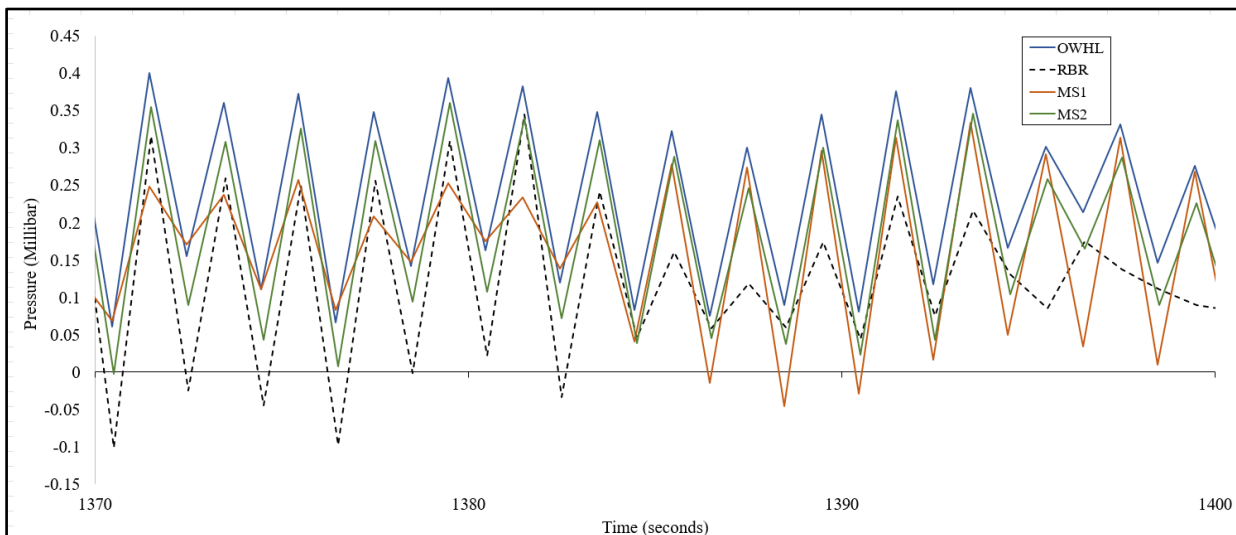


Figure 12: Initial pressure readings from simulated wave activity of MS2, MS1 and OWHL, all compared against readings of the RBR commercial sensor.

Table 2: Significant wave height measurements from commercial grade RBR, compared with constructed sensors.

Sensor	Full Depth (m)	Wave Height Large (m)	Wave Height Small (m)	Weak Wave Set (m)
RBR-TWR2050	1.55	0.71	0.44	0.02
MS1	1.69	0.80	0.49	0.01
MS2	1.61	0.75	0.46	0.02
OWHL	1.64	0.77	0.46	0.02

5.2 Sensor Deployment

Sensors were mounted on 24.95kg deck blocks outfitted with eye hooks manually inserted into two opposing corners via hammer drill. The sensors were placed between the eye hooks and held to the deck block by zip ties tightened at the front and back end of the housing. Sensors were then placed in three transects on a 60-meter shoreline at 5 meters (used as a control) 20 meters and 45 meters; while extending offshore into the water at 2 meters, 4 meters, 6 meters, 8 meters and 10 meters.

5.3 Artificial Vegetation Deployment

Slalom poles were chosen to serve as artificial vegetation due to their ability to anchor in the ground by a metal spike but still move freely at the base via spring. The poles were 167.64 cm tall and 2.54cm in diameter. The initial test was modelled with natural spacing and stem density variations from *Scirpoides holoschoenus*, whose stem density measures around 150 plants per m². This means that there is 8.3 cm between each plant. Our slalom poles had a 2.54 cm diameter,

meaning that 40 cm spacing between each pole would be required to mimic natural *Scirpoides holoschoenus* growth characteristics.



Figure 13: Day 1 vegetation array and spacing from 8:00 am to 12:10 pm 09/06/2021.

5.3.1 Day Four Data

After each day of deployment data was reviewed to assess any attenuation by the array spacing of that day. An increase in attenuation was observed as the vegetation spacing was placed at smaller intervals. The vegetation stems were approximately 2.54 cm wide which allowed for 10cm spacing when placed as close as possible. The wave direction of this day was occurring at a northwest angle relative to the transects which led to the decision to move the 45 meters transect beside the 20 meters transect. Approximately 40 poles were placed alongside and in front of transect 2, and 40 were placed alongside and in front of transect 3 (Figure 14). When spaced at 10cm intervals, the vegetation remained anchored for longer periods during high boat wake activity. This led to using pressure transducer data from the fourth day configuration only. As previously mentioned, stems containing adequate rigidity and higher stem density result in higher

attenuation capabilities (Anderson et al. 2011). With the artificial vegetation placed at smaller intervals more resistance for the wake was created, leading to dispersion of the wake's energy.

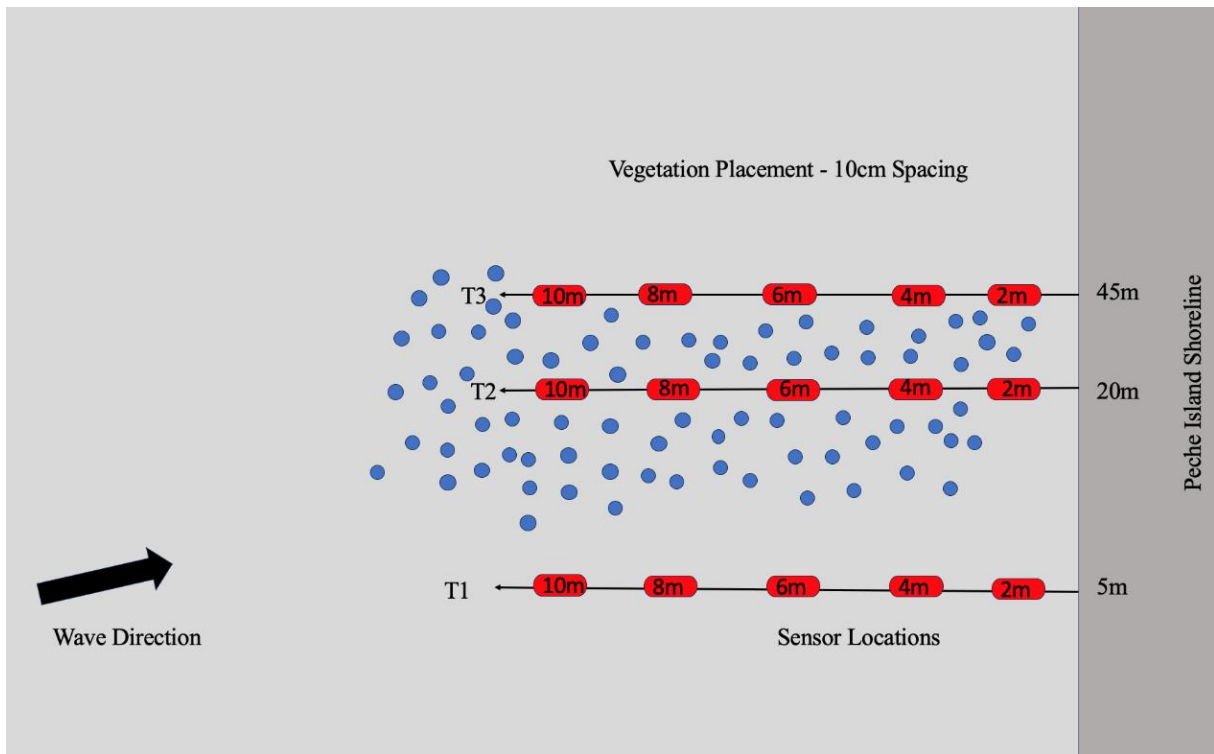


Figure 14: A planform representation of the vegetation array on day 4 of collection showing transect placement, sensor spacing, vegetation spacing, and wake direction.

5.4 Vessel Monitoring

Observable vessel features were recorded (I.e., vessel type and direction), along with the time they passed the research area shoreline and the time of their resulting wake. Vessel information such as speed, draft length and name was recorded with the mobile application 'Marine Traffic.' Which serves as a real-time map with vessel information for that area. Both the field data and app data were later combined and used as a reference against any outstanding wave activity seen during initial data analysis. This allowed for simple assumptions to be made regarding the wave forcing of different vessels on the Peche Island shoreline. When marine traffic was absent in the shipping channel, the vessel RV Haffner was used by the research team to generate boat

wake activity in front of the experimental setup by driving back and forth at varying speed intervals.

5.5 Data Analysis

The data were extracted from the pressure sensors, and correction factors were applied to account for inconsistencies in depth measurements (compared to the RBR TWR-2050) within the sensor readings. Atmospheric pressure was determined at the collection site by dedicating one sensor to record continuously on shore. By monitoring changes in atmospheric pressure, predictions can be made about the potential wave heights that may result from these wind patterns (Lyman et al. 2020). Atmospheric pressure was subtracted from the sensor's raw, absolute pressure readings to yield gauge pressures as a function of time. A zero-crossing method was applied to isolate wave groups relative to crest and trough heights, and a statistical analysis of the resultant wave heights and periods was performed. Statistical analysis of wave heights noted the maximum height, average wave period and max wave period within the entirety of a full day of collection.

Wave energy for each burst sample was estimated to the first order using index wave height and period with the following formula:

$$H_i = \frac{2U_m}{\sqrt{g/h}} \quad (6)$$

Where g is the acceleration of gravity, h is still water depth, and U_m is the maximum near-bottom orbital velocity, which is the sum of the maximum wave height, the local water depth, and the wavelength. Use of the index wave height allowed for the relative comparison of wave packets over time, and between various vessels. Index values highlight data trends and changes that might not be apparent when looking at raw data (Figure 15).

Index wave height was then applied to a variation of the wave energy equation to obtain Energy Density E :

$$E = \frac{1}{8}(\rho)(g)(H_i^2) \quad (7)$$

Where ρ is density of water, g is the acceleration of gravity and H_i is the index wave height. Energy density reveals the amount of energy concentrated within a unit area of the water's surface due to the wave motion. Waves with higher wave heights will have higher energy densities. Significant wave heights were then obtained from cumulative pressure readings to compare alongside calculated wave index. The significant wave height was defined as the average of the highest one-third of the waves. The use of significant wave parameters is based on the relationship of Equation 7, meaning that larger waves contain more energy and can provide a more representative measure of the erosive potential of the local wave climate.

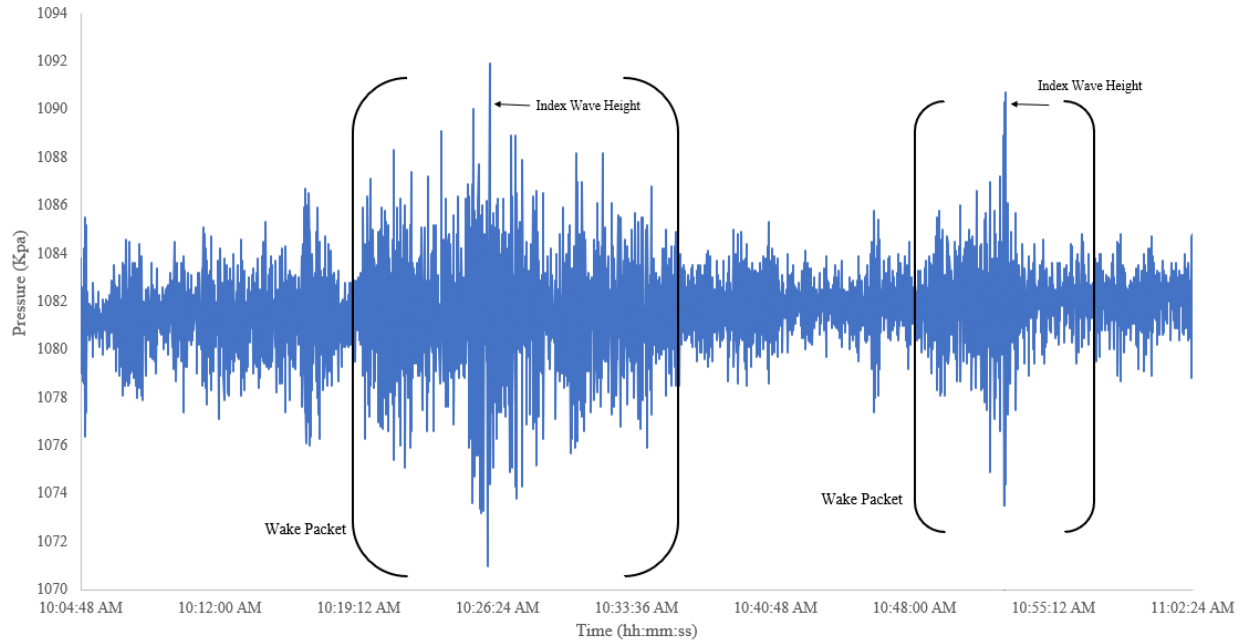


Figure 15: Data from September 6/2023 of a burst sample of isolated boat wakes used to calculate Index Wave Height. Wake times were cross-referenced with in field notes of vessel passages.

Wave attenuation was then estimated using an exponential decay function from Kobayashi et al. (1993).

$$\frac{H_n}{H_i} = e^{(-D_t x)} \quad (8)$$

where D_t is the total decay coefficient through the marsh and x is the horizontal distance between gages. H_n is the significant wave height at gage n . H_i is index wave height. The total decay coefficient estimates combined wave attenuation by vegetation and wave breaking. To isolate vegetation influence Equation 8 was modified to Equation 9.

$$\frac{H_i K_v}{H_i} = e^{(-D_v X)} \quad (9)$$

where K_v is the vegetation coefficient, and D_v is the decay coefficient for the vegetation. Incident wave height occurring in both the numerator and denominator serve as a model of the change in

K_v throughout the vegetation array. Decay coefficients were calculated by plotting the results from Equation 3 and applying a trendline equation to the distribution.

Wave attenuation in shallow water wave energy can be guided by numerous parameters such as reflection, diffraction, refraction, and transmission. Accounting for each of these parameters was not possible for this study due to equipment restraints and time. Therefore, the influence of these parameters is neglected, and Equation 10 is applied to quantify wave attenuation with consideration for vegetation, shoaling and breaking when appropriate:

$$H_n = K_v K_s H_i \quad (10)$$

where H_n is wave height at gage n (n=1-5), K_v is the vegetation transmission coefficient, K_s is the shoaling coefficient, and H_i is the index wave height. To determine the shoaling coefficient K_s , wave group celerity at both the incident wave gage and gage of concern were calculated as:

$$K_s = \sqrt{\frac{Cg_i}{Cg_n}} \quad (11)$$

where Cg_i is the wave group celerity (wave speed) at the incident gage, and Cg_n is the wave group celerity at the gage of concern. Shoaling is defined as the gradual decrease in the energy and change in height of waves as they propagate over a distance. The interaction of the wave with the seabed in shallow waters creates bottom friction, which can impact the propagation of the wave. This friction can lead to changes in the wave period. Shorter wavelengths (higher frequencies) are more influenced by shallow waters and slow down more than waves of longer wave lengths (lower frequencies). This differential slowing of different frequencies can lead to changes in the overall wave shape and slight modifications of the wave periods. Therefore, to measure the wave characteristics at shore it is important to consider the effects of shoaling has on wave attenuation, especially when measured through vegetation (Bryan et al., 2020). To assess wave attenuation differences across the three distinct transects, ANOVA was used for its effectiveness in comparing

means among multiple groups, making it well-suited for evaluating potential variations in wave attenuation. The ANOVA test is then applied to analyze whether there are significant differences in wave attenuation means among the three transects on both a wake and wave to wave basis.

5.6 Drag Coefficients

To estimate the amount of energy dissipation (ε_v) due to vegetation, drag coefficients (C_D) were estimated by measuring the time-averaged rate of wave energy dissipation:

$$\varepsilon_v = \frac{2}{3p} r C_D b N \left(\frac{kg}{2\sigma}\right)^3 \frac{\sinh^3 kh_r + 3\sinh kh_r}{3k \cosh^3 kh} H^3 \quad (12)$$

where b_v is the blade thickness and N is the density of vegetation, k is the wave number, H is the wave height, g is the acceleration due to gravity, ρ is the density of water. This equation does not account for the reflection that would be induced by vegetation (Mendez et al. 1999), it also assumes that the horizontal velocity of the vegetation is smaller than the orbital velocity, in that the vegetation can be assumed rigid while imparting a large drag force on the waves (Houser et al. 2014).

The variation in drag coefficient was plotted against the Reynolds number (Re), with the dependency of C_D on Re described as:

$$C_D = \alpha + \left(\frac{\beta}{Re}\right)^\gamma \quad (13)$$

where α , β , and γ are the constant, coefficient, and exponent of the fitted relationship. Because the Reynolds number does not include a measure of stiffness, it cannot account for the effects of stem flexibility. Therefore, a comparison of the data collected by Houser et al. (2014) is done to

demonstrate how stem flexibility affects the overall relationship between the drag coefficient and the Reynolds number.

5.7 Design Density

The estimated C_D for the vegetation allows for design densities to be estimated based on a design/target wave height at the shoreline. Specifically, defining ε_v as the difference in the wave energy offshore and the target wave height at the shoreline, and rearranging Equation 12, allow for the design vegetation density to be estimated. For the purposes of this study, the design wake height at the shoreline is assumed to be that of the annual average wind-wave height at the shoreline. The western side of Peche Island has a fetch length of ~ 1.1 km, while average wind speeds during the summer shipping period are 14 km h^{-1} from the west and south. This means that waves are fetch-limited and that average heights are 0.06 m with periods of ~ 1.0 s.

6. Results

To assess the potential for artificial vegetation to attenuate waves, it is important to use a clear and distinguishable wake train. In this respect, a total of 25 vessel passages were recorded on September 9th, 2021, but only 3 out of the 25 vessel passes were chosen for calculations. Selection of the three vessels was done after the day of data was extracted, it was then graphed with corresponding times that were then cross referenced with field notes for recorded vessel passages and their associated wake arrival on shore. Vessel information was then extracted from the mobile app. Vessels containing the clearest representation of wakes were selected for analysis (Figure 17). The Freighter ‘Laurentien’ will be referred to as ‘Freighter 1’ and is a single hull with a gross tonnage of 10,897kg, contained a length of 222.5m, and width of 23m, and operated ~ 804 m from the Peche shoreline at 9.5kn. The Freighter ‘Niagara’ will be referred to as ‘Freighter 2’ and is a

single hull with a gross tonnage of 10,878kg, contained a length of 222.51m, and a width of 23.76m and operated ~804m from the Peche Shoreline at 9.9kn. The RV Haffner was used to transport the field team and equipment to Peche Island but was also used to test attenuation effects of the vegetation from vessels operating at closer distances and with higher wake periods (faster operating speeds). The RV Haffner is a 7.92m length and 2.56m wide aluminum vessel weighing 1769kg dry. It was equipped with dual 70 horsepower engines. The RV Haffner made 19 passes perpendicular to the transects, at only ~ 20 meters offshore, with varying speeds between 15-19 kn. On this sampling day, the vegetation array was placed at a 45-degree angle to account for the primary angle of wake approach on that day (Figure 14). Wind speed averaged at 15.19 km/h, which was the lowest for the four days of data collection, and the winds on that day were from the northwest. The maximum wind-wave heights and periods for the sampling period are presented in Table 4.

Table 4: Sensor depths along with measured background wind-wave heights and periods for each transect.

Transect	Sensor	Sensor Depth (m)	Avg wind- wave Height (cm)	Max wind-wave Height (cm)	Avg wind-wave Period (s)	Max wind-wave Periods (s)
1	S7	0.56	2.58	5.09	2.58	8.10
1	S8	0.64	2.35	4.58	2.58	8.10
1	S9	0.80	2.31	5.60	2.40	6.94
1	S10	0.80	2.43	5.29	2.43	10.41
1	S6	0.84	2.27	4.38	2.57	10.42
2	S12	0.46	2.54	5.40	2.78	8.10
2	S17	0.30	2.64	4.99	2.63	9.25
2	S13	0.68	2.54	5.91	2.57	6.94
2	S4	0.38	2.39	4.58	2.69	8.10
2	S16	0.71	2.41	4.38	2.57	5.78
3	S18	0.51	2.53	3.56	2.61	4.62
3	S15	0.74	2.35	5.09	2.50	6.94
3	S3	0.65	2.31	4.68	2.63	10.41
3	S14	0.88	2.31	5.80	2.34	6.94
3	S5	0.81	2.34	3.56	2.57	13.8

Wind wave heights and periods were calculated for the periods immediately before the wake arrival to determine the background wave activity and isolate the vessel wakes (Table 4). Because wind waves contain smaller wave heights over longer periods of time, they can be useful for extracting specific vessel wakes in extensive plots of data (Figure 15). The wind data and calculations were not used specifically for attenuation analysis, but the combined effects of wind energy and boat wake energy can have substantial effects on shorelines, however accounting for both was outside the scope of this study.

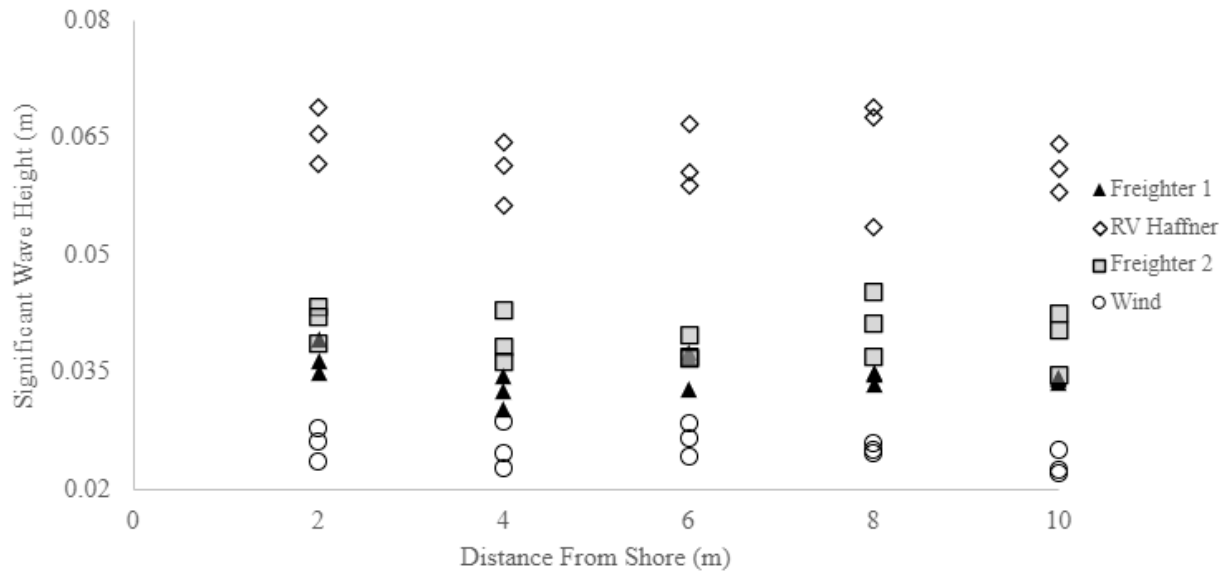


Figure 16: Example plot of H_s comparing wind wake energy and boat wake energy across transects.

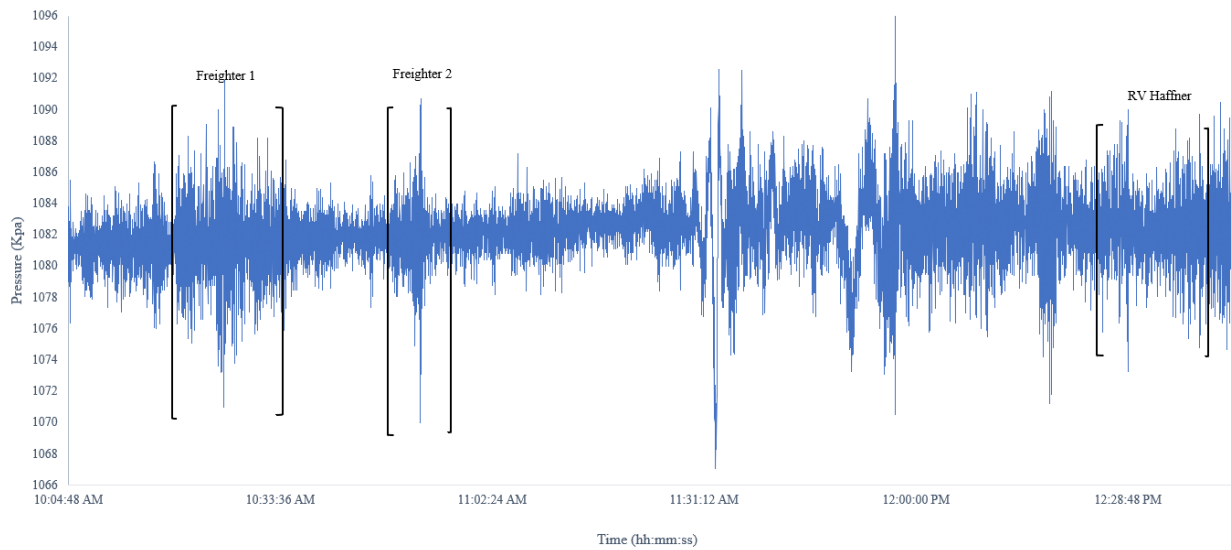


Figure 17: Pressure readings from day four's data containing values from all 15 sensors, with selected boat wakes notated.

6.1 Wake Heights

Day four of data collection contained 25 recorded vessel passages but only three wake packets from three separate vessels could be isolated and used for attenuation analysis: 2 freighter vessels (freighter 1 and freighter 2), who both contributed one pass from the Detroit River, and the RV Haffner who continuously passed in front of the vegetation array ~ 16 times at 20 meters offshore. An ANOVA test revealed that significant wave heights for freighters were significantly lower than that of the RV Haffner ($p < 0.001$), which is most likely due to the closer sailing line and high operating speed of the RV Haffner. The significant wave height (H_s) measured on all transects from the outer and inner sensors revealed an increasing trend for the wakes produced by the RV Haffner as the wave approached the shoreline, suggesting that the waves were shoaling. Shorter wavelengths (higher frequencies) like that produced by the RV Haffner are more influenced by shallow waters and slow down more than waves of longer wave lengths (lower frequencies). The smaller waves generated by the freighters did not exhibit a clear trend across transect 1, suggesting that shoaling was not balanced by wakes of longer periods or that energy dissipation of the freighter wakes occurred sooner and further offshore. Transect 2 contained a variation between the freighter wakes with freighter 2 experiencing a decreasing trend in wave height, and freighter 1 containing a slight increase in wave height (Figure 18).

While transect 3 reveals a sharp increase in wake height for freighter 2, and relatively little change in freighter 3 the overall wake heights are lower than transect 1, suggesting that wake attenuation did occur, but only in the presence of vegetation. The interaction of the wave with the seabed in shallow waters creates bottom friction, which can impact the propagation of the wave. This differential slowing of different frequencies can lead to changes in the overall wave shape and slight modifications of the wave periods. Therefore, to measure the wave characteristics at

shore it is important to consider the effects of shoaling has on wave attenuation, especially when measured through vegetation (Bryan et al., 2020).

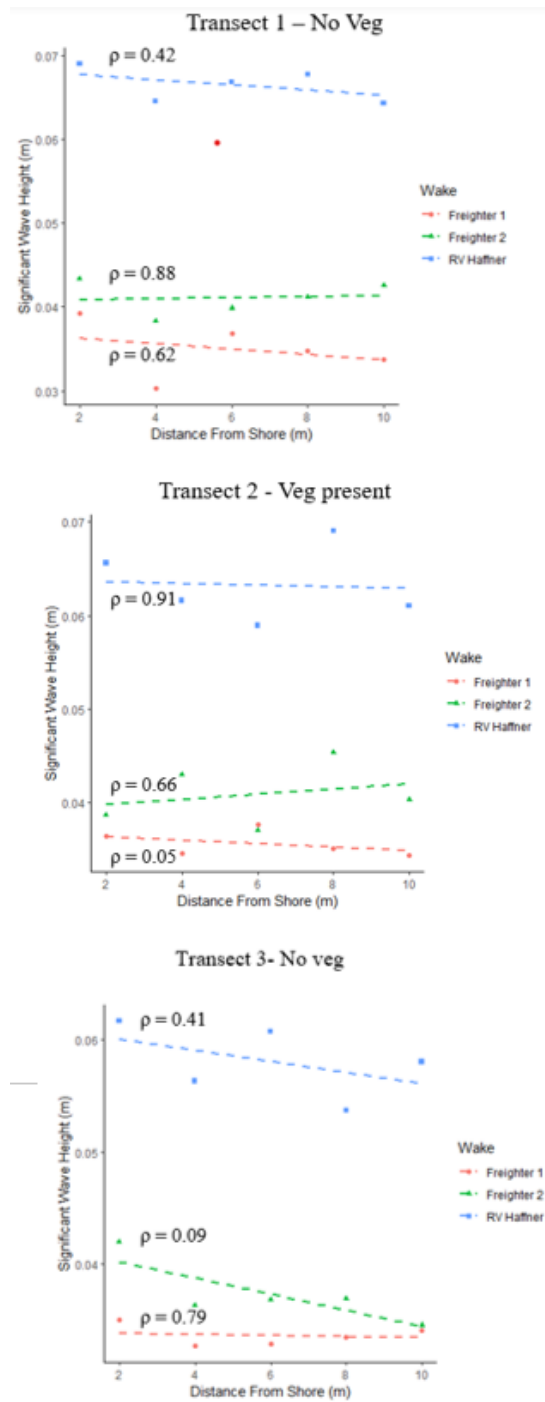


Figure 18: Significant wave heights (in meters) for all three transects for each wake. The first sensor in each transect occurs at 2m offshore and continues out into the river to 10m.

6.2 Wave Shoaling

The shoaling coefficient (Equation 10) was applied to index wave heights for each vessel wake to remove the effects of wave shoaling on their transformation across the transects. Removing the effects of shoaling highlight the attenuation of the wave field across transect 2 and 3. It can be seen in Figure 20 that transect 1 decayed at a faster rate than transect 3 in all wakes, but Anova tests between all three transects and then wakes revealed that transect 2 had significantly lower Deshoaled wave heights ($p < 0.001$) than transects 1 and 3, while the RV Haffner contained significantly lower deshoaled values when compared to freighter 1 and 2. In order to determine the effect of the vegetation, the control decay contributed by transect 1 needed to be removed. The result of this subtraction provides a more accurate estimate of the intrinsic or natural decay processes, in other words, it helps determine how quickly wave energy decays under normal conditions, without the interference of external factors.

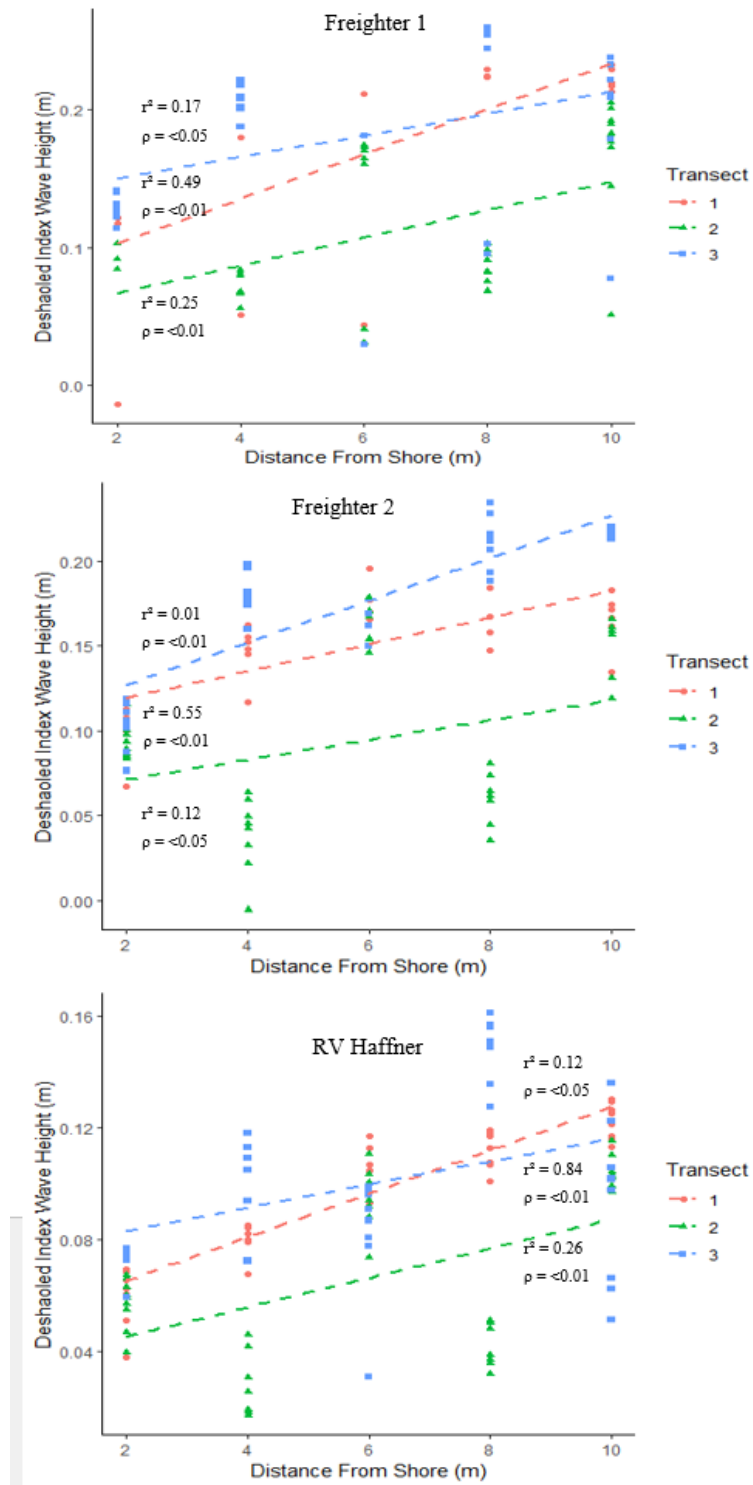


Figure 19: Deshaoled wave heights (in meters) for all three transects for wakes from Freighter 1, 2 and the RV Haffner. The first sensor in each transect occurs at 2m offshore and continues out into the river to 10m. Note that Transect 2 contains significantly lower wave heights in each wake.

6.3 Decay Coefficients

After subtracting deshoaled index wave height values of transect 1 from both transects 2 and 3, the decay coefficients for each wake and transect could be plotted (Figure 20). Decay coefficients are useful for quantifying the decrease in wave energy as it approaches the shoreline, and by comparing the amount of decay occurring between both wakes and transects, this allows for comparison of numerous factors influencing attenuation by the vegetation. An ANOVA test revealed that there were no significant differences between the individual wakes, but significant differences between each transect were present. Transect 2 had significantly higher average decay values than transect 1 ($p < 0.01$), while transect 3 had significantly lower average decay values than transect 2 ($p < 0.01$). There was no significant difference between transect 1 and 3, although transect 3 had higher median values than transect 1 (Table 5).

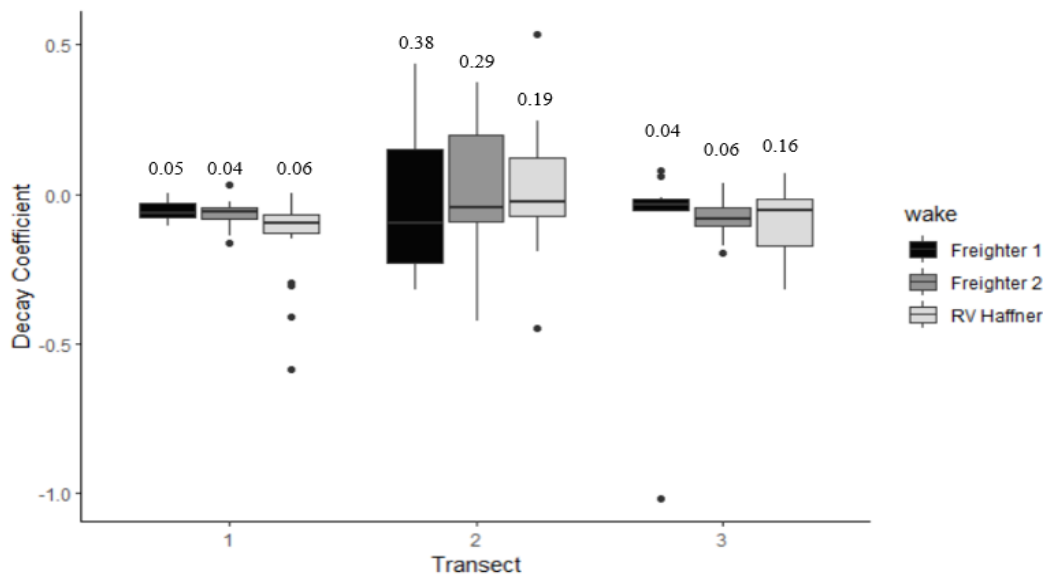


Figure 20: Box plots containing mean, min and max distributions of decay rates in all three wakes, along with interquartile ranges for each wake and transect. All values are in cm.

Table 5: List of Decay Coefficient mean, median, min and max values organized by wake and transect.

Transect	Wake	Median (cm)	Median of Wake(cm)	Median of Transect(cm)	Mean (cm)	Min (cm)	Max (cm)
1	Freighter 1	-0.0644	-0.074	-0.068	-0.0563	-0.1048	0.0039
1	Freighter 2	-0.0570	-0.062		-0.0629	-0.1647	0.0326
1	RV Haffner	-0.0963	-0.052		-0.1336	-0.5865	0.0047
2	Freighter 1	-0.0580		-0.034	-0.0215	-0.3209	0.4324
2	Freighter 2	-0.0435			-0.0347	-0.4251	0.3729
2	RV Haffner	-0.0767			-0.0228	-0.4508	0.5338
3	Freighter 1	-0.0341		-0.057	-0.1076	-1.0180	0.0801
3	Freighter 2	-0.0849			-0.0813	-0.1971	0.0355
3	RV Haffner	-0.0534			-0.0860	-0.3204	0.0676

On a wave-by-wave basis, positive maximum decay coefficients occur throughout each wake (Table 5). After aligning each positive value by time and transect, transect 2 contained the most positive values (21) with transect 3 containing 7 positive values and transect 1 containing 3 positive values. The RV Haffner, while operating at ~16kph contained the most positive values out of all the wakes (13). The deshoaled values in Figure 20 show transect 2 containing the lowest wave heights, however once the data is separated to a wave-by-wave basis its revealed that decay did not occur sequentially over the entire wake, and this is especially true for the RV Haffner, who contained the lowest median averages of decay (indicating less attenuation). The positive decay values from the RV Haffner could be explained through the closer operating speed and the higher frequency wakes. As mentioned above, the RV Haffner remained in plowing mode as it passed in front of the vegetation array, meaning that the bow wave formed from plowing mode created a steady state short period wake (Table 6). Despite the positive values occurring mostly within the passes by the RV Haffer, indicating less attenuation capability for these conditions, the mean values of the decay coefficients for all 3 wakes indicate that a decay in wave energy occurred, but

was experienced least by the RV Haffner (Table 5). Furthermore, the presence of rigid vegetation can modify the undertow current velocities and increase wave setup within a surf zone, potentially contributing to the positive decay values experienced by transect 2.

Table 6: Average wave periods for each wake and transect, note that the RV Haffner contains the shortest wave period values.

Vessel	Transect	Wake Period Average by Transect(s)	Wake Period Average (Entire)(s)
Freighter 1	1	2.59	2.57
Freighter 1	2	2.56	
Freighter 1	3	2.53	
RV Haffner	1	2.51	2.50
RV Haffner	2	2.52	
RV Haffner	3	2.49	
Freighter 2	1	2.85	2.76
Freighter 2	2	2.68	
Freighter 2	3	2.80	

6.4 Drag Coefficient (C_D)

Previously published data from field and laboratory studies (Kobayashi et al. 1993; Mendez et al 1999; Mendez and Losada 2003; Augustin et al. 2009; Bradley and Houser 2009; Paul and Amos 2011; Stratigaki et al. 2011, Houser et al. 2014) was used to compare the variation of the C_D against Reynolds Numbers (Re). Results are presented in Figure 21. When compared to the previous studies, the drag coefficients for all 3 wakes calculated in the present study reveal a higher order of magnitude in drag forces over the range of Reynolds numbers. Visual observations reveal clustering between the Freighter wakes, whose Reynolds numbers average at 9166.40 for Freighter

1 with drag coefficients averaging at 106.97, Freighter 2 contained a Reynolds number average of 9819.81 and a drag coefficient average of 86.87. The RV Haffner contained a Reynolds number average of 6516.53, and a drag coefficient average of 139.40.

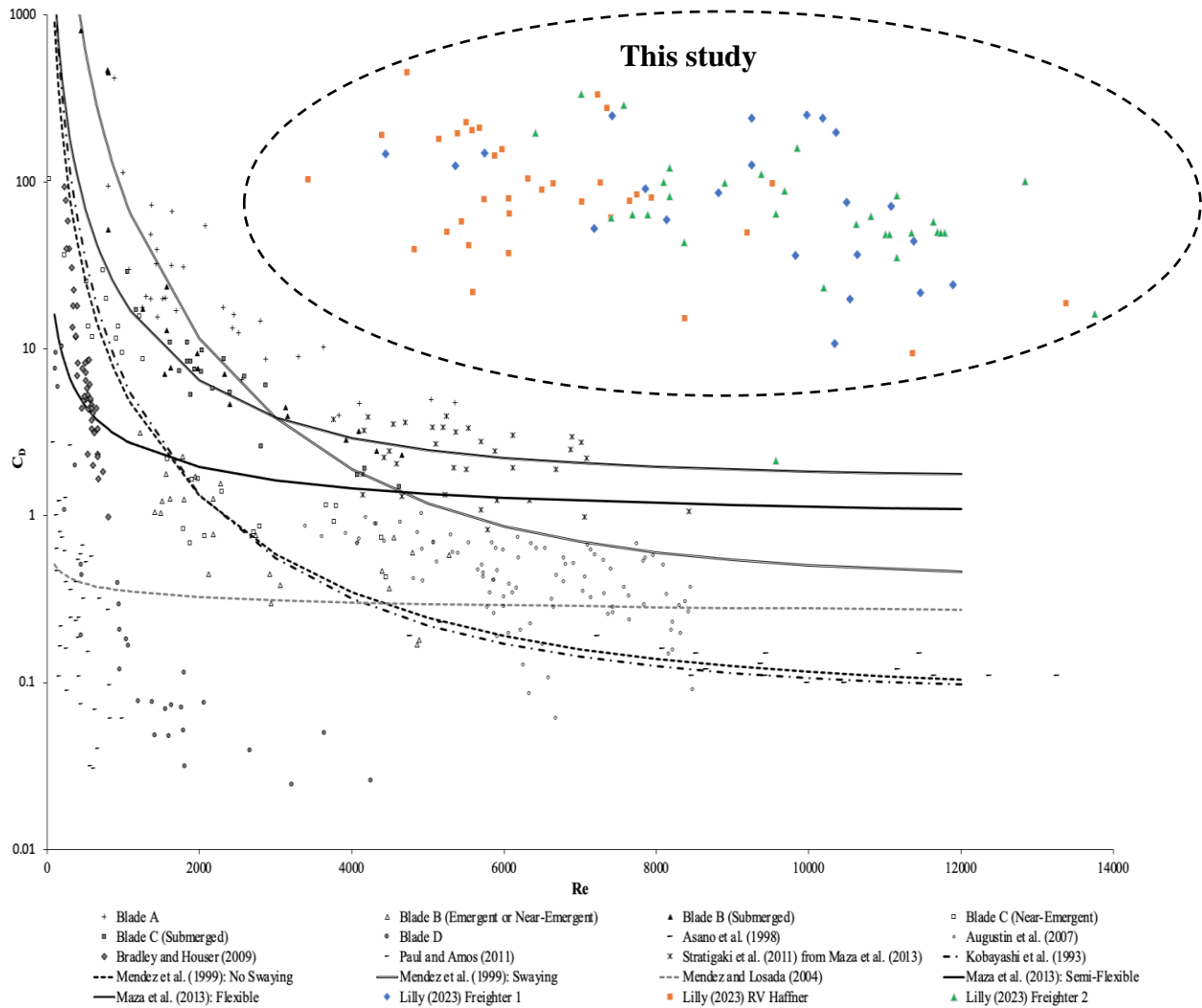


Figure 21: Drag coefficient values for all three wakes (circled in black) plotted against the Reynolds values revealing little similarity to the characteristic C_d and Re relationship presented in the data from Bradley & Houser (2014).

Table 7: Drag coefficient and Reynolds number averages and ranges for all three wakes.

Vessel	Drag Coefficient	Reynolds Number	Range (Re)	Range (C_D)
Freighter 1	106.97	9166.40	7449.24	241.92
Freighter 2	140.00	6516.53	13395.70	909.53
RV Haffner	86.87	7449.24	7341.09	333.34

The vegetation of the present study does not show the characteristic C_D to Re relationship that is presented in the Bradley & Houser (2014) study (Figure 21). There is little variation in the drag for all 3 wakes as the Reynolds value increases. The drag coefficient averages for the present study are most like the drag coefficients of the artificial vegetation used in the Bradley & Houser (2009) study; blades A & B (submerged). Reynolds numbers from the Augustin et al (2007) study reveal similar plotted Reynolds values but contain lower drag coefficients in comparison, resulting in a similar decay curve once plotted (Figure 21). Regression analysis of the wakes was performed on Transects 2 and 3 of each wake, however results revealed that neither the transect patterns or densities varied significantly enough to contribute to the overall drag coefficient and Reynolds number relationship. When compared to studies conducted using living vegetation like Asano et al. (2007) & Paul & Amos (2011), the drag coefficient values for the present study reveal higher values overall. The Reynolds numbers for the Asano et al. (1998) study is clustered near the 4000 values, which exhibits a similar trend to the Reynolds value of this study.

6.5 Design Density Estimate:

The decay rates of the attenuated wave heights are based on the Drag Coefficients for a piece of vegetation and its density. Once the Drag Coefficient is calculated, Equation 8 can be rearranged to determine the vegetation density required to achieve a wave decay of <0.05 m at the shoreline to then be consistent with the background wind-wave heights (0.06 m):

$$N = \frac{Ev}{2/3\pi} (\rho)(C_D)(d)\left(\frac{(l)(9.81)/2(2\pi)}{T}\right)^3 (s) \quad (11)$$

Where N = vegetation density, ρ is density of water, C_D is the drag coefficient, d is artificial vegetation diameter, l is wave number, T is wave period and s is seconds. N was calculated for each wake to yield the average number of poles required to attenuate waves to <0.05m.

To achieve a wave decay of <0.05 m Freighter 1 required a vegetation density of $N= 2.30\text{m}^2$, while Freighter 2 required a density of $N= 2.51\text{m}^2$, and the RV Haffner requiring a density of $N= 3.20\text{m}^2$. The artificial vegetation used in the current study cost ~\$15.00 per stalk and were used along 60 m of shoreline to 10 m offshore. Extending the vegetation along the entire length of Peche Island (1.124km) at the design density would require ~33,720 stems at a cost of ~\$505,800.00. The rock walls at the northeastern shoreline extended only 680 m across the island. This means that a design density of ~20,400 stems at a cost of ~\$306,000.00 is required to effectively provide attenuation at the same magnitude as the revetment project along the Peche Island Shoreline. This does not include the cost of installation with buried anchor or maintenance. As this is an untested technology, it is not clear what frequency of maintenance would be required.

7. Discussion

Shoreline erosion is an increasingly significant challenge to coastal management in Canada (Brampton 1992, Othman 1994, Turker et al. 2006), as it can impact developmental decisions by landowners and governments. Marshes and vegetated shorelines can dampen wave energy and storm surge by providing more bank stability (Nepf, 2012). Through the processes described above, aquatic vegetation provides ecosystem services with an estimated annual value of over 10 trillion dollars (Nepf, 2012). And with the looming threat of climate change causing more frequent high-intensity storms, the need for low- cost nature-based solutions deserve to be explored (Anderson et al. 2014). Consequently, recent nature-based trends in coastal engineering are focusing on non-intrusive forms of shoreline protections, such as vegetation, which can help reduce accelerated erosion from wind waves and boat wakes.

Attenuation of waves and wakes depends on characteristics of the plant such as geometry (Mendez & Losada, 2004), buoyancy (Koch et al. 2006), density (Nepf, 1999), stiffness (Ghisalberti & Nepf,2002), and spatial configurations (Fonseca et al. 1982), in addition to the characteristics of the waves (Nepf, 2012). While there have been several studies to examine wind wave attenuation through vegetation (Mendez & Losada,1999, Camfield, F.E. 1977), the ability of vegetation to attenuate vessel-generated wakes has received limited attention. Whereas wind wave fields tend to be quasi steady in the distribution of height and period, boat wakes are characterized by decreasing height and period due to the dispersion of the wake away from the sailing line (Galmore, 2008). While the generation of vessel generated waves (i.e., boat wakes) are mostly understood (Croad & Parnell, 2002), the characteristics of the wake at the shoreline varies based on the size and shape of the vessel, the way it is being operated (planing vs displacement) and the distance from the sailing line, meaning that the distribution of height and period at the shoreline

can be quite variable (Croad & Parnell, 2002). Given that attenuation varies in response to the relative movement of the vegetation with the wave, it is reasonable to assume that the attenuation of an unsteady wake may be different than a quasi-steady wind wave field. The purpose of this study is to test the attenuation capability of artificial vegetation within the Detroit River. Specifically, results suggest that the drag coefficient (C_D) of the artificial vegetation was greater than previously studied natural and artificial vegetation under quasi-steady waves (Figure 21). The higher drag coefficient and the lack of a relationship with the Reynolds number (Re) suggests that drag was largely independent of the wake flow around the poles, possibly because of how the vegetation pivoted with each wave. While further study is required to assess the specific motion of the vegetation with the passage of a wake, the larger C_D across a range of wave motion suggests that is a potentially effective design characteristic for using vegetation at the shoreline.

7.1 Index Wake Height and Decay Coefficient

An ANOVA test revealed that significant wave heights for freighters were significantly lower than that of the RV Haffner ($p < 0.001$). This is most likely due to the short distance from shore (as compared to the Freighters who operated in the shipping lanes of the Detroit River) and the fact that the RV Haffner did not enter planning mode during the test cycles, indicating that the artificial vegetation was not able to attenuate sufficiently for these conditions. In shallow water, the redistribution of wave energy can be caused by shoaling, but also wave breaking, reflection, diffraction, and refraction. However, the ability to account for each of these factors is beyond the scope of this study. A shoaling coefficient was applied to the significant wave heights for each wake, which accounted for the natural and varying depth of the shoreline. Most of the previous studies have been performed in either laboratory settings or model simulation, which allows for

shoaling to be accounted for or eliminated. Transect 2 contained significantly lower deshoaled wave heights than transects 1 & 3. Due to the incoming wave direction moving northwest relative to the transects, wave attenuation would have occurred over transect two before transect three, with transect three experiencing wave energy after initial attenuation from transect 2. Transect 1 did show the highest correlation between deshoaled wave height and distance from shore, while also decreasing in wave height at a faster rate than transect 2; both of these findings influenced the decision to subtract the decay rates of transect 1 from both transect 2 and 3. However, without a full bathymetric profile, the higher correlation between deshoaled wave height and distance from shore (despite lack of vegetation) in transect one cannot be fully quantified, only estimated. The measured sensor depths of Transect 1 continuously increase with depth as they move offshore, unlike the values in transect 2 and 3 (See Table 2); this could potentially explain the higher correlation between deshoaled wave height and distance from shore seen in transect 1.

The interquartile ranges of the decay coefficients for all three wakes are represented in box plots in Figure 21 and reveal that the decay coefficients of transect 1 and 3 contain similar ranges as in the Bradley & Houser (2008) study, whose results state that the exponential decay coefficient ranged from 0.004 to 0.02 with an average coefficient of 0.01. However, in transect 2 decay coefficients for each wake increase substantially, indicating that the least attenuation occurred on this transect. Bradley & Houser (2008) found that the variation in the decay coefficient of the seagrass appears to depend on the Reynolds number; stating that wave attenuation decreased as incident wave height increased and conditions became more turbulent ($200 < Re < 800$). Video observations showed seagrass blades swaying over the entire wave cycle when exposed to lower orbital velocities; however, at higher orbital velocities the blades would become streamlined into the flow of water, leading to reduced drag and attenuation. The blades were also found to move

in-phase with waves at a lower frequency (0.38 Hz) but out of-phase with higher peak frequency waves (0.67 Hz) (Bradley & Houser, 2008). This would suggest that the higher frequencies (shorter wave periods) in a spectrum should experience more attenuation by seagrass; results which are supported by Lowe et al. (2007). The passes of the RV Haffner produced wakes at higher speeds with shorter wave periods as compared to the freighters, which is most likely because the RV Haffner remained in plowing mode as it passed in front of the vegetation array, meaning that the bow wave formed from plowing mode created a steady state short period wake (Table 6). The RV Haffner also experienced the least amount of decay of all three wakes, indicating that the emergent rigid vegetation was not able to attenuate at higher frequency conditions. Furthermore, the high rigidity and stem diameter of the vegetation could have introduced stem- scale turbulence, contributing to the lack of decay seen for the higher energy conditions. Vortex generation occurs within stem- scale turbulence, draining energy from the mean flow (or canopy drag). If this vortex generation is 100% efficient, then the rate at which turbulent energy is produced is equal to the rate of work done by the flow against canopy drag (Nepf, 2012). In other words, the hydrodynamics acting on the vegetation in combination to the rigidity and diameter could have contributed to the decrease in wave energy decay. Over a horizontal bed, wave attenuation is the sole hydrodynamic process, whereas over a sloped bed, wave attenuation is in competition with wave shoaling affecting wave breaking, as well as wave setup, wave runup and wave- generated currents (Chalmoukis et al. 2023).

7.2 Drag Coefficients

The drag coefficients of the artificial vegetation in the present study were relatively large and exhibited little variation compared the drag coefficients to the previous studies plotted in the Houser et al, (2014) study (Figure 21). The relative lack of variation of C_D with Re suggests that the flexible vegetation has a smaller drag coefficient compared to the rigid vegetation, with the difference between the two being consistent between all studies (Houser et al. 2014). When observing submerged vegetation with semi-flexible blades, video analysis suggested that the flexing of the blade is smaller than the orbital diameter, due to the weaker orbital velocities at depth being unable to overcome the inertia of the blades. (Houser et al. 2014).

The results of this study reveal a similar distribution of C_D values that do not vary with changes in Re and can be attributed to hydrodynamic parameters acting on the vegetation. The Reynolds number defines hydrodynamic length scale in terms of vegetation diameter, while parameters such as relative wave height, submergence ratio, wave steepness and Froude number are functions of the hydrodynamic parameters only. This indicates that the diameter of rigid vegetation is an important predictor for wave- vegetation interaction and controls flow, where flexible vegetation follows flow (Veelen et al. 2020). Furthermore, the velocity structure of waves does not follow linear wave theory components in the presence of vegetation, and the magnitude of velocity attenuation and the direction and position of net currents differ between rigid and flexible vegetation (Veelen et al. 2020). Specifically, the interaction between waves and rigid vegetation creates a current in the direction of wave propagation through the vegetation which impedes the flow of water, causing a significant reduction in downstream flow velocity. Meaning that vegetation containing higher rigidity like the one from the current study can be used as an appropriate model for wave attenuation.

The similar data curvature (Figure 21) in this study and the artificial vegetation study of Augustin et al. (2007) study suggests that similar wave conditions acted on the vegetation, or that the vegetation behaved the same way over a range of wave conditions. The higher drag coefficients of this study can be attributed to the stem length (emergence) and stem diameter of the vegetation implemented, and potentially further quantified through the rigidity parameter, which can be derived by relating the drag coefficient to the ratio of the blade rigidity to the oscillatory velocity as a proxy of the drag force. In other words, the rigidity parameter can predict the drag coefficient and wave attenuation for vegetation when they contain similar morphology, but different degrees of flexibility. While drag coefficients mostly depend on blade morphology and vertical structures of the canopy, it's reasonable to assume that the relationship between drag coefficient and Reynolds number is dependent on flexibility. Because the drag coefficient has a dependency on the rigidity parameter, it could be used to estimate energy dissipation by vegetation when given blade morphology and canopy structure (Houser et al. 2014). Given that the C_D is calculated based directly on the energy dissipation, it is independent of the relative velocity of the vegetation. In this respect, the Re values are overestimated by a factor of 10 and that the flex of the stalk is ~90% of the orbital velocity independent of the size of the wave. This may reflect the behaviour of the spring at the base of the stalk and represent an interesting opportunity for additional research on how artificial vegetation structure and design can influence wave attenuation.

When comparing the drag coefficient of this study to that of living vegetation, both Asano et al. (1998) and Paul & Amos (2011) contain much lower C_D values, indicating less attenuation capability. However, the drag coefficient and Reynolds number curvature for the Paul and Amos (2011) study does follow the decreasing trend seen in most of the previously plotted data in Figure 21, which can be most likely attributed to the extensive intertidal vegetation field tested and given

that all deployments contained no higher than approximately $\sim 0.3\text{m}$ wave heights (Paul and Amos, 2011). The decrease in the drag coefficient as Reynolds values increase which is seen in previous studies is due to the separation of flow behind the vegetation stalk. At low velocities (low Reynolds values) water attaches to the stalk and there is no current generated, resulting in higher drag coefficients. As velocities increase (high Reynolds value), water particles begin to separate from the stalk creating a wake of turbulence, which results in lower drag coefficients (Nepf, 2012).

The vegetation of this study retains high drag coefficient values regardless of flow, but the pivoting of the spring base along with high rigidity and wide stem diameter may provide some insight into the results. The amount of useful flexibility is dependent on the vegetation type and density. The reduced wave attenuation capacity seen in entirely flexible vegetation is due to swaying, which reduces the frontal area of the vegetation, thereby limiting the total work that can be done by the drag force. Swaying motions also reduce the relative velocity between water and vegetation when vegetation sways with the flow, and for submerged vegetation this results in amplified horizontal particle velocity above the vegetation canopy and reduced velocities within the vegetation which is also called in- canopy flow. Furthermore, a return current develops high in the water column when the vegetation is sufficiently submerged, and the magnitude of the current and the amplification depend on the submergence ratio (van Veleen et al. 2020). Further testing would be needed to isolate these conditions for emergent rigid vegetation. Clearly there is a need for further investigation of how the drag coefficient and Reynolds number relationship is affected by the blade and stem morphology. Due to the difficulty in comparing vegetation data across studies conducted in various environments and containing different blade and stem arrays; the clustering of drag coefficient relationships by vegetation type must be observed. Further study is required to assess the specific motion of the vegetation specifically with wakes, but the larger C_D

across a range of wave motion suggests that the vegetation would serve as a potentially effective design characteristic as a nature- based solution at the Peche Island shoreline.

7.3 Artificial Vegetation as an Alternative to Hard Engineering Structures

Due to both strong river currents and heavy wave action from vessel traffic, Peche Island has decreased in area by ~ 20% since 1931, leading to commitments from government entities to conduct the largest restoration project on the Canadian side of the Detroit River (DRCC, 2022). To manage erosion, over 5,605 tonnes of stone and rock were placed along the northeast shoreline, creating a 600- meter- long revetment wall, while 11,785 tonnes of material was used to construct nine offshore sheltering islands. The revetment wall consisted of gabion stone, filter fabrics and armour rock and contributed to \$1,152,199.20 in costs to the restoration project, while \$2,062,171 in additional expenses was required for the offshore islands. (K. Money, personal communication, ERCA,2023). As with all rock structures on shorelines, the rock size, face slopes, crest elevation and crest width must be considered. Revetment rock size is dependent on incident wave heights, periods, and direction, where the structure crest elevation must be above wave run- up limit during high- energy conditions to provide shoreline protection. Trying to incorporate revetment with adequate functionality, aesthetic and recreational preferences can often lead to increased cost and considerations when personal property is in jeopardy (e.g., materials, labor costs, permitting fees, engineering designs and landscaping, among others).

The artificial vegetation used in the current study cost ~\$15.00 a piece and were used across the shoreline for 60 meters, while extending into the river for 10 meters; however, the rock revetment project implemented at Peche Island spreads as far as 200 meters across the northeastern shore (DRCC, 2022). As mentioned earlier, Equation 11 was used to determine vegetation density

requirements to achieve a wave decay of $<0.05\text{m}$. Results showed that for Freighter 1 $N= 2.30\text{m}^2$, Freighter 2 $N= 2.51\text{m}^2$, and for the RV Haffner $N= 3.20\text{m}^2$. This means that for every meter square of shoreline, at least 3 pieces of artificial vegetation are required for wave attenuation of <0.05 meters; and to account for the total project length across shore and into the water $\sim\$300,000$ worth of vegetation would be required. This does not include the cost of installation with buried anchor or maintenance. As this is an untested technology, it is not clear what frequency of maintenance would be required. The Detroit River has served an important role in the history of Detroit and Windsor and is considered one of the world's busiest waterways due to shipping and trading (Jacobs & Lytwyn, 2020). A total of 18 Freighters and 83 personal vessels ranging in size from fishing boats to yachts were recorded during the data collection days. This does not serve as a realistic representation of traffic passing near Peche Island as data recording stopped once instruments were removed from the water each day; however, it's clear the Peche Island shoreline is subjected to high frequency boat traffic and will continue to erode without some form of protection. The vegetation used for the present study contained a high amount of C_D , and the lack of relationship with the Re suggests that the drag was independent of the wake flow around the poles, possibly because of how the vegetation pivoted with each wave. Unlike some other structures, such as submerged objects or solid barriers, which can create turbulent wake flows that persist downstream, emergent, and more rigid vegetation tends to create less turbulent wake flows (Veelen et al. 2020). This is because stems sway with the water flow, allowing water to pass through more smoothly. As a result, the vegetation's impact on the flow downstream is less disruptive, and it doesn't create strong vortices or turbulence behind the stalk, leading to less overall drag.

8. Conclusions

An in-field experiment using semi-rigid artificial vegetation was conducted to quantify the ability of vegetation to attenuate vessel-generated waves. The study was conducted at Peche Island, which is eroding due to a combination of wind-waves, lack of lake ice during the winter and many vessel-generated waves. The artificial vegetation used for the current study did provide vessel wake attenuation, however, the mode of operation for the vessel and therefore resultant wake did contribute to the vegetations attenuation capabilities. The C_D of the artificial vegetation was greater than previously studied natural and artificial vegetation under quasi-steady waves. The associated motion of the vegetation in response to the wake is believed to play a large role in the higher drag afforded by this vegetation. The lack of relationship with the Reynolds number suggests that the wake flow around the poles remained turbulent which afforded high amounts of drag. Furthermore, the high surface area of the vegetation stem could have contributed to flow dispersion within the canopy.

These findings represent an important design characteristic for the future of nature-based solutions along shorelines. Artificial vegetation allows for the mitigation of erosion problems, but the physical and overall economic performance of the vegetation is site specific, and therefore dependent on design parameters. There is anecdotal evidence to suggest that boat wakes are attenuated by vegetation from the field (Ismail et al. 2017) and the laboratory (Manis et al. 2015), there have been no studies to quantify the ability of vegetation to attenuate unsteady wave trains (e.g., wakes) and quantify the associated C_D of the vegetation. Such measurements can provide insight for coastal managers to better protect shorelines from erosion using vegetation as a living (nature-based) shoreline, or by identifying wake restrictions to limit shoreline impacts based on the extent, density, and type of vegetation. Implementation of the artificial vegetation along the

Peche Island shoreline would cost ~\$300,000 for the vegetation alone, while costs for maintenance and installation are undeterminable at this time.

References

- Ahmad, M. F., Yusoff, M. M., Husain, M. L., Nik, W. W., & Muzathik, A. M. (2011, July). An investigation of boat wakes wave energy: a case study of Kemaman river estuary. In *Universiti Malaysia Terengganu International Annual Symposium. UMTAS, Kuala Terengganu* (pp. 907-913).
- Augustin, L.N., Irish, J.L. and Lynett, P., 2009. Laboratory and numerical studies of wave damping by emergent and near-emergent wetland vegetation. *Coastal Engineering*, 56(3), pp.332-340.
- Anderson, M.E. and Smith, J.M., 2014. Wave attenuation by flexible, idealized salt marsh vegetation. *Coastal Engineering*, 83, pp.82-92.
- Baldwin, D.S., 2008. Impacts of recreational boating on riverbank stability: Wake characteristics of powered vessels
- Bilkovic, D.M., Mitchell, M., Davis, J., Andrews, E., King, A., Mason, P., Herman, J., Tahvildari, N. and Davis, J., 2017. Review of boat wakes wave impacts on shoreline erosion and potential solutions for the Chesapeake Bay.
- Bradley, K. and Houser, C., 2009. The relative velocity of seagrass blades: Implications for wave attenuation in low-energy environments. *Journal of Geophysical Research: Earth Surface*, 114(F1).
- Brampton AH. (1992). Engineering significance of British saltmarshes. In *Saltmarshes: Morphodynamics, 966 Conservation, and Engineering Significance*, ed. JRL Allen, K Pye, Cambridge University Press, p. 115– 967 122
- Bryan, K. R., & Power, H. E. (2020). Wave behaviour outside the surf zone. In *Sandy Beach Morphodynamics* (pp. 61-86). Elsevier.
- Camfield, F.E. 1977. A method for estimating wind-wave growth and decay in shallow water with high values of bottom friction. CETA 77-6. Fort Belvoir, VA: Coastal Engineering Research Center.
- Dawes, C. J., Andorfer, J., Rose, C., Uranowski, C., & Ehringer, N. (1997). Regrowth of the seagrass *Thalassia testudinum* into propeller scars. *Aquatic Botany*, 59(1-2), 139-155.
- Dean, B. and Bhushan, B., 2010 Shark-skin surfaces for fluid-drag reduction in turbulent flow: a review *Phil. Trans. R. Soc. A*.3684775–4806
- Douglas, S. L., & Pickel, B. H. (1999). The tide doesn't go out anymore! –bulkheading our urban bay shorelines. *Shore & Beach*, 67, 19-25.

- Eriksson BK, Sandström A, Isaeus M, Schreiber H, Karås P. 2004. Effects of boating activities on aquatic vegetation in the Stockholm archipelago, Baltic Sea. *Estuar Coast Shelf S.* 61(2):339–349. doi:10.1016/j.ecss.2004.05.009.
- Fonseca, M.S., J.S. Fisher, J.C. Zieman, and G.W. Thayer. 1982. Influence of seagrass, *Zostera marina* L., on current flow. *Estuarine, Coastal, and Shelf Science.* 15: 351-364.
- Fonseca, M. S., and J. A. Calahan (1992), A preliminary evaluation of wave attenuation by four species of seagrass, *Estuarine Coastal Shelf Sci.*, 35, 565 – 576.
- Fonseca, M. S., and M. A. R. Koehl (2006), Flow in seagrass canopies: The influence of patch width, *Estuarine Coastal Shelf Sci.*, 67, 1–9.
- Galvin, C. J. (1972). Wave breaking in shallow water. *Waves on beaches and resulting sediment transport*, 413-456.
- Gittman, R.K., J. Fodrie, A.M. Popowich, D.A. Keller, J.F. Bruno, C.A (Collective Agreement). Currin, C.H. Peterson, and M.F. Piehler. 2015. Engineering away our natural defences: an analysis of shoreline hardening in the US. *Frontiers in Ecology and the Environment* 13: 301-307.
- Glamore, W.C. 2008. A Decision support tool for assessing the impact of boat wake waves on inland waterways. *International Conference on Coastal and Port Engineering in Developing Countries.* 20 p. Retrieved from: <http://pianc.org>.
- Ghisalberti, M., and H. M. Nepf (2002), Mixing layers and coherent structures in vegetated aquatic flow, *J. Geophys. Res.*, 107(C2), 3011, doi:10.1029/2001JC000871.
- Grizzle, R. E., F. T. Short, C. R. Newell, H. Hoven, and L. Kindlom (1996), Hydrodynamically induced synchronous waving of seagrasses: ‘Monami’ and its possible effects on larval mussel settlement, *J. Exp. Mar. Biol. Ecol.*, 206, 165–177.
- Hager, W. H., & Castro-Orgaz, O. (2017). William Froude and the Froude number. *Journal of Hydraulic Engineering*, 143(4), 02516005.
- Hallac, D. E., Sadle, J., Pearlstine, L., Herling, F., & Shinde, D. (2012). Boating impacts to seagrass in Florida Bay, Everglades National Park, Florida, USA: links with physical and visitor-use factors and implications for management. *Marine and Freshwater Research*, 63(11), 1117-1128.

- Houser, C., 2010. Relative importance of vessel-generated and wind waves to salt marsh erosion in a restricted fetch environment. *Journal of Coastal Research*, 26(2), pp.230-240.
- Houser, C., Trimble, S. and Morales, B., 2014. Influence of blade flexibility on the drag coefficient of aquatic vegetation. *Estuaries and coasts*, 38(2), pp.569-577.
- Ismail, Isfarita, Mohd Lokman Husain, and Rozaimi Zakaria. "Attenuation of waves from boat wakes in mixed mangrove forest of rhizophora and bruguiera species in matang perak." *Malaysian Journal of Geosciences (MJG)* 1, no. 2 (2017): 29-32.
- Jadhav, R.S., Chen, Q. and Smith, J.M., 2013. Spectral distribution of wave energy dissipation by salt marsh vegetation. *Coastal Engineering*, 77, pp.99-107.
- Knutson, P.L., Brochu, R.A., Seelig, W.N. and Inskeep, M., 1982. Wave damping in *Spartina alterniflora* marshes. *Wetlands*, 2(1), pp.87-104.
- Kobayashi, N., Raichle, A.W. and Asano, T., 1993. Wave attenuation by vegetation. *Journal of waterway, port, coastal, and ocean engineering*, 119(1), pp.30-48.
- Koch, E. W. (2002). Impact of boat-generated waves on a seagrass habitat. *Journal of Coastal Research*, 66-74.
- Koch, E. W., Sanford, L. P., Chen, S. N., Shafer, D. J., & Smith, J. M. Waves in Seagrass Systems: Review and Technical Recommendations. 2006.
- Lyman, T.P., Elsmore, K., Gaylord, B., Byrnes, J.E. and Miller, L.P., 2020. Open Wave Height Logger: An open-source pressure sensor data logger for wave measurement. *Limnology and Oceanography: Methods*, 18(7), pp.335-345.
- Manis, J. E., Garvis, S. K., Jachec, S. M., & Walters, L. J. (2015). Wave attenuation experiments over living shorelines over time: a wave tank study to assess recreational boating pressures. *Journal of coastal conservation*, 19, 1-11.
- MacDonald, N.J., 2003, October. Numerical modelling of coupled drawdown and wake. In *Proc Canadian Coastal Conf* (pp. 15-17).
- Mendez, F.J., I.J. Losada, and M.A. Losada. 1999. Hydrodynamics induced by wind waves in a vegetation field. *Journal of Geophysical Research* 104(8): 18383–18396
- Mendez, F. J., and I. J. Losada (2004), An empirical model to estimate the propagation of random breaking and nonbreaking waves over vegetation fields, *Coastal Eng.*, 51, 103–118.

- Möller, I. (2006). Quantifying saltmarsh vegetation and its effect on wave height dissipation: Results from a UK East coast saltmarsh. *Estuarine, Coastal and Shelf Science*, 69(3-4), 337-351.
- Moëller, I., J. R. French, D. J. Legget, and M. Dixon (1999), Wave transformation over salt marshes: A field and numerical modeling study from North Norfolk, England, *Estuarine Coastal Shelf Sci.*, 49, 411–426.
- Möller, I., Kudella, M., Rupprecht, F., Spencer, T., Paul, M., Van Wesenbeeck, B. K., ... & Schimmels, S. (2014). Wave attenuation over coastal salt marshes under storm surge conditions. *Nature Geoscience*, 7(10), 727-731.
- Mork, M. (1996), The effect of kelp on wave damping, *Sarsia*, 80, 323 – 327.
- Mosisch TD, Arthington AH. 1998. The impacts of power boating and water skiing on lakes and reservoirs. *Lakes Reserv Res Manage.* 3(1):1–17. doi:10.1111/j.1440-1770.1998.tb00028.x.
- National Research Council (NRC). 2007. *Mitigating Shoreline Erosion along Sheltered Coasts*. Washington D.C.: The National Academies Press, 188 p.
- Nepf, H.M. 1999. Drag, turbulence, and diffusion in flow through emergent vegetation. *Water Resources Research*. 35(2): 479-489.
- Nepf, H.M. 2004. Vegetated flow dynamics. In: Fagherazzi, S., Marani, M., Blum, L. (Eds.). *Ecogeomorphology of Tidal Marshes*, *Coastal and Estuarine Studies*, 59: 137–164
- Neumeier, U.R.S. and Amos, C.L., 2006. The influence of vegetation on turbulence and flow velocities in European saltmarshes. *Sedimentology*, 53(2), pp.259-277.
- Ozeren, Y., Wren, D.G. and Wu, W., 2014. Experimental investigation of wave attenuation through model and live vegetation. *Journal of Waterway, Port, Coastal, and Ocean Engineering*, 140(5), p.04014019.
- Othman, M.A. (1994). Value of mangroves in coastal protection. *Hydrobiologia*, 285, 277-282.
- Parnell, K.E., McDonald, S.C. and Burke, A.E., 2007. Shoreline effects of vessel wakes, Marlborough Sounds, New Zealand. *Journal of Coastal Research*, pp.502-506.

- Passaro, M., Hemer, M. A., Quartly, G. D., Schwatke, C., Dettmering, D., & Seitz, F. (2021). Global coastal attenuation of wind-waves observed with radar altimetry. *Nature Communications*, 12(1), 3812.
- Paul, M. and Amos, C.L., 2011. Spatial and seasonal variation in wave attenuation over *Zostera noltii*. *Journal of Geophysical Research: Oceans*, 116(C8).
- Rapaglia, J., Zaggia, L., Ricklefs, K., Gelinis, M., & Bokuniewicz, H. (2011). Characteristics of ships' depression waves and associated sediment resuspension in Venice Lagoon, Italy. *Journal of Marine Systems*, 85(1-2), 45-56.
- Ricketts, P., and P. Harrison. 2007. Coastal and ocean management in Canada: moving into the 21st Century. *Coastal Management* 35: 5–22.
- Shepard, C. C., Crain, C. M., & Beck, M. W. (2011). The Protective Role of Coastal Marshes: A Systematic Review and Meta-analysis. *PLoS ONE*, 6(11), e27374
- Sheremet, A., Gravois, U. and Tian, M., 2013. Boat-wake statistics at Jensen Beach, Florida. *Journal of waterway, port, coastal, and ocean engineering*, 139(4), pp.286-294.
- Shuster, R., Sherman, D.J., Lorang, M.S., Ellis, J.T. and Hopf, F., 2020. Erosive potential of recreational boat wakes. *Journal of Coastal Research*, 95(SI), pp.1279-1283.
- Silinski, A., Heuner, M., Schoelynck, J., Puijalon, S., Schröder, U., Fuchs, E., ... & Temmerman, S. (2015). Effects of wind waves versus ship waves on tidal marsh plants: a flume study on different life stages of *Scirpus maritimus*. *PloS one*, 10(3), e0118687.
- Soomere, T., 2007. Nonlinear components of ship wake waves.
- Stumbo, S., K. Fox, F. Dvorak, and L. Elliot. 1999. The prediction, measurement, and analysis of wake wash from marine vessels. *Marine Technology* 36: 248-260.
- Temple, N.A., Webb, B.M., Sparks, E.L. and Linhoss, A.C., 2020. Low-cost pressure gauges for measuring water waves. *Journal of Coastal Research*, 36(3), pp.661-667.
- Tonelli, M., Fagherazzi, S. and Petti, M., 2010. Modeling wave impact on salt marsh boundaries. *Journal of geophysical research: Oceans*, 115(C9).
- Tschirky, P., Hall, K. and Turcke, D., 2001. Wave attenuation by emergent wetland vegetation. In *Coastal Engineering 2000* (pp. 865-877).

- Turker, U., Yagci, O., Kabdasli, M. (2006). Analysis of coastal damage of a beach profile under the 1287 protection of emergent vegetation. *Ocean Engineering*, 33, 810-828
- US Army Corps of Engineers, USGS. (n.d) *Discharge Measurements- The Detroit River*. Availableat: <https://www.lre.usace.army.mil/Missions/Great-LakesInformation/Outflows/Discharge-Measurements/Detroit-River/> (Accessed: 23/11/21).
- van Veelen, T. J., Fairchild, T. P., Reeve, D. E., & Karunarathna, H. (2020). Experimental study on vegetation flexibility as control parameter for wave damping and velocity structure. *Coastal Engineering*, 157, 103648.
- Williams, S. L. (1988). *Thalassia testudinum* productivity and grazing by green turtles in a highly disturbed seagrass bed. *Marine Biology*, 98(3), 447-455.
- Wu, W.C. and Cox, D.T., 2015. Effects of wave steepness and relative water depth on wave attenuation by emergent vegetation. *Estuarine, Coastal and Shelf Science*, 164, pp.443-450.
- Yang, S. L., Shi, B. W., Bouma, T. J., Ysebaert, T., & Luo, X. X. (2012). Wave attenuation at a salt marsh margin: a case study of an exposed coast on the Yangtze Estuary. *Estuaries and Coasts*, 35, 169-182.
- Yousefi, R., Shafaghat, R. and Shakeri, M., 2013. Hydrodynamic analysis techniques for high-speed planing hulls. *Applied ocean research*, 42, pp.105-113.
- Zhang, W., Ge, Z. M., Li, S. H., Tan, L. S., Zhou, K., Li, Y. L., ... & Dai, Z. J. (2022). The role of seasonal vegetation properties in determining the wave attenuation capacity of coastal marshes: Implications for building natural defenses. *Ecological Engineering*, 175, 106494.

Vita Auctoris

NAME: Jamie Kathryn Lilly

PLACE OF BIRTH: Clarksdale, Mississippi, United States of America

YEAR OF BIRTH: 1991

EDUCATION: Lee Academy High School, Clarksdale, Mississippi, USA
2005-2009

Texas A&M University- Galveston, Galveston, Texas, USA
2015-2019, B.Sc.

University of Windsor, Windsor, Ontario, CA
2020 – 2023, M.Sc.